



NAVAL POSTGRADUATE SCHOOL

MONTEREY, CALIFORNIA

THESIS

**ESTIMATIONS OF ATMOSPHERIC CONDITIONS FOR
INPUT TO THE RADAR PERFORMANCE SURFACE**

by

Frank D. Price Jr.

December 2007

Thesis Advisor:
Co-Advisor:

Kenneth L. Davidson
Peter S. Guest

Approved for public release; distribution is unlimited

THIS PAGE INTENTIONALLY LEFT BLANK

REPORT DOCUMENTATION PAGE			<i>Form Approved OMB No. 0704-0188</i>	
Public reporting burden for this collection of information is estimated to average 1 hour per response, including the time for reviewing instruction, searching existing data sources, gathering and maintaining the data needed, and completing and reviewing the collection of information. Send comments regarding this burden estimate or any other aspect of this collection of information, including suggestions for reducing this burden, to Washington headquarters Services, Directorate for Information Operations and Reports, 1215 Jefferson Davis Highway, Suite 1204, Arlington, VA 22202-4302, and to the Office of Management and Budget, Paperwork Reduction Project (0704-0188) Washington DC 20503.				
1. AGENCY USE ONLY (Leave blank)		2. REPORT DATE December 2007	3. REPORT TYPE AND DATES COVERED Master's Thesis	
4. TITLE AND SUBTITLE Estimations of Atmospheric Conditions for Input to the Radar Performance Surface			5. FUNDING NUMBERS	
6. AUTHOR(S) Frank D. Price Jr.				
7. PERFORMING ORGANIZATION NAME(S) AND ADDRESS(ES) Naval Postgraduate School Monterey, CA 93943-5000			8. PERFORMING ORGANIZATION REPORT NUMBER	
9. SPONSORING /MONITORING AGENCY NAME(S) AND ADDRESS(ES) N/A			10. SPONSORING/MONITORING AGENCY REPORT NUMBER	
11. SUPPLEMENTARY NOTES The views expressed in this thesis are those of the author and do not reflect the official policy or position of the Department of Defense or the U.S. Government.				
12a. DISTRIBUTION / AVAILABILITY STATEMENT Approved for public release; distribution is unlimited			12b. DISTRIBUTION CODE	
13. ABSTRACT (maximum 200 words) <p>This study addresses the support of non-acoustic ASW operations by timely atmospheric and ocean surface descriptions on features that impact radar and electro-optical sensor systems. The first part of this study is an analysis of meteorology and oceanography (METOC) data collected off Wallops Island, VA. A second part is a description of data and procedures applied in a "Proof of Concept" for a Radar Performance Surface developed and executed at NPS for the Pacific Fleet exercise Valiant Shield 2007 for periscope detection. In both field experiments NPS employed METOC instruments and personnel in theater to collect in situ "truth" data for the ocean and atmosphere.</p> <p>Evaluated are the sensitivities of the parameters that serve as the input to the performance surface. Surface parameters as predicted by the Navy's Coupled Ocean Atmosphere Mesoscale Prediction System (COAMPS®) are compared to in-situ data to assess the sensitivities of air-sea temperature differences and relative humidity errors on predictions of ducting, super and sub-refractive conditions.</p> <p>Addressed are atmospheric measurement techniques, use of climatology and numerical modeling as the input to the Radar Performance Surface. This study evaluates the degree of which mesoscale models can accurately predict the true predicted propagation conditions based on comparisons with in situ data. A statistical summary shows COAMPS® data has sufficient skill when compared to in situ data.</p>				
14. SUBJECT TERMS METOC, COAMPS®, ASW, Radar Performance Surface, Wallops Island, Valiant Shield			15. NUMBER OF PAGES 81	
			16. PRICE CODE	
17. SECURITY CLASSIFICATION OF REPORT Unclassified	18. SECURITY CLASSIFICATION OF THIS PAGE Unclassified	19. SECURITY CLASSIFICATION OF ABSTRACT Unclassified	20. LIMITATION OF ABSTRACT UU	

THIS PAGE INTENTIONALLY LEFT BLANK

Approved for public release; distribution is unlimited

**ESTIMATIONS OF ATMOSPHERIC CONDITIONS FOR INPUT TO THE
RADAR PERFORMANCE SURFACE**

Frank D. Price Jr.
Lieutenant, United States Navy
B.S., Norfolk State University, 2000

Submitted in partial fulfillment of the
requirements for the degree of

MASTER OF SCIENCE METEOROLOGY AND PHYSICAL OCEANOGRAPHY

from the

**NAVAL POSTGRADUATE SCHOOL
December 2007**

Author: Frank D. Price Jr.

Approved by: Kenneth L. Davidson
Advisor

Peter S. Guest
Co-Advisor

Philip A Durkee
Chairman, Department of Meteorology

THIS PAGE INTENTIONALLY LEFT BLANK

ABSTRACT

This study addresses the support of non-acoustic ASW operations by timely atmospheric and ocean surface descriptions on features that impact radar and electro-optical sensor systems. The first part of this study is an analysis of meteorology and oceanography (METOC) data collected off Wallops Island, VA. The second part is a description of data and procedures applied in a “Proof of Concept” for a Radar Performance Surface developed and executed at NPS for the Pacific Fleet exercise Valiant Shield 2007 for periscope detection. In both field experiments NPS employed METOC instruments and personnel in theater to collect in situ “truth” data for the ocean and atmosphere.

The sensitivities of the parameters that serve as the input to the performance surface are evaluated. Surface parameters as predicted by the Navy’s Coupled Ocean Atmosphere Mesoscale Prediction System (COAMPS[®]) are compared to in-situ data to assess the sensitivities of air-sea temperature differences and relative humidity errors on predictions of ducting, super and sub-refractive conditions.

Atmospheric measurement techniques, use of climatology and numerical modeling as the input to the Radar Performance Surface are addressed. This study evaluates the degree of which mesoscale models can accurately predict the true predicted propagation conditions based on comparisons with in situ data. A statistical summary shows COAMPS[®] data has sufficient skill when compared to in situ data.

THIS PAGE INTENTIONALLY LEFT BLANK

TABLE OF CONTENTS

I.	INTRODUCTION.....	1
A.	MOTIVATION	1
B.	APPLICATION.....	3
II.	BACKGROUND	5
A.	ATMOSPHERE CONDITIONS AND REFRACTION.....	5
1.	Introduction.....	5
2.	Refractivity	6
3.	Super-Refraction.....	8
4.	Trapping layer and the Evaporation Duct	8
5.	Sub-refraction	11
B.	REFRACTIVITY FROM BULK SURFACE LAYER MODELS	12
C.	HIGH RESOLUTION COAMPS®	17
D.	SATELLITE DATA.....	20
E.	PROPAGATION EFFECTS MODEL APPLICATION, APM	20
III.	WALLOPS ISLAND 2000 FIELD EXPERIMENT	23
A.	INTRODUCTION.....	23
1.	Purpose.....	23
2.	Naval Postgraduate School Flux Buoy	24
B	“TRUTH”/BUOY DATA COLLECTION	25
1.	Mean Environmental and Turbulent Data Collection System	25
C.	BULK PARAMETERIZATION PROCESSING FOR WALLOPS 2000.....	26
1.	The Near-Surface Layer Scaling Parameters: Profile Properties and Evaporation Duct Height	26
IV.	VALIANT SHIELD 2007 “PROOF OF CONCEPT” FOR RADAR PERFORMANCE SURFACE	27
A.	FIELD COLLECTION	27
B.	DEVELOPMENT OF THE RADAR PERFORMANCE SURFACE	28
C.	COMPARISON OF VALIANT SHIELD 2007, COAMPS® DATA AND BULK DATA FOR EVAPORATION DUCT	30
V.	RESULTS FROM TRUTH VERSUS CLIMATOLOGY & COAMPS® COMPARISONS.....	33
A.	COMPARISONS OF DATA SOURCES APPLIED TO NPS BULK MODEL	33
1.	Comparison of Wallops Island NPS Buoy and Climatology Data	33
2.	Comparison of Wallops Island NPS Buoy, COAMPS® Data and Evaporation Duct.....	38
B.	METEOROLOGICAL SITUATION FOR MAY 11, 2000	44

C.	PROPAGATION RESULTS	51
VI.	SUMMARY AND CONCLUSION	57
A.	SUMMARY	57
B.	CONCLUSION	57
	LIST OF REFERENCES.....	59
	INITIAL DISTRIBUTION LIST	63

LIST OF FIGURES

Figure 1.	CNMOC Battlespace on Demand. CONOPS for Naval Oceanography.....	2
Figure 2.	Integrated Approach for Data Source	4
Figure 3.	Refraction Categories.....	8
Figure 4.	Profiles for a Standard Atmosphere.....	9
Figure 5.	Plot of a typical vertical modified refractivity profile with corresponding evaporation duct height and trapping layer. From: (Frederickson et al., 2000b).....	10
Figure 6.	Plot of model computed evaporation duct heights versus model input air – sea temperature differences, computed with wind speed (U) = 2 m/s, T_{sea} = 12 °C and different values of relative humidity as indicated. From: (Frederickson, 2000b).....	14
Figure 7.	Plot of model computed evaporation duct heights versus model input air – sea temperature differences, computed with wind speed (U) = 5 m/s, T_{sea} = 12 °C and different values of relative humidity as indicated. From: (Frederickson, 2000b).....	15
Figure 8.	Plot of model computed evaporation duct heights versus model input air – sea temperature differences, computed with wind speed (U) = 10 m/s, T_{sea} = 12 °C and different values of relative humidity as indicated. From: (Frederickson, 2000b).....	16
Figure 9.	Spatial display of NPS Buoy, COAMPS® and Climatology grid points.....	17
Figure 10.	Propagation regions in the Advanced Propagation Model (Hitney, H. V., 1994)	21
Figure 11.	NPS Flux Buoy	24
Figure 12.	Infrared Radiation Pyrometers, model KT15.82, Wintronics 2007.....	28
Figure 13.	Flow Diagram for producing the Radar Performance Surface	29
Figure 14.	8 August to 14 August 2007 RV Cory Chouest in-situ (blue) and COAMPS® time series (red dots) comparisons for air temperature (T_{air}), sea surface temperature (SST), wind direction (Wind Dir) and pressure (P).....	31
Figure 15.	8 August to 14 August 2007 RV Cory Chouest in-situ (blue) and COAMPS® (red) time series comparisons for evaporation duct height (EDH), ASTD (T_{air} -SST), relative humidity (RH) and wind speed (Speed).....	31
Figure 16.	5 April to 13 May 2000 NPS Buoy (blue) and Climatology (black) time series comparisons for air temperature (T_{air}), SST (T_{sea}), wind direction (WD) and pressure (PR).....	34
Figure 17.	5 April to 13 May 2000 NPS Buoy (blue) and Climatology (black) time series comparisons for evaporation duct height (EDH), ASTD (T_{air} - T_{sea} IR), Wind Speed (WS) and Relative Humidity (RH).	35
Figure 18.	5 April to 13 May 2000 NPS Buoy and climatology scatter plot and time series comparisons for air temperature (T_{air}).....	36

Figure 19.	5 April to 13 May 2000 NPS Buoy and climatology scatter plot and time series comparisons for SST (Tsea).	36
Figure 20.	5 April to 13 May 2000 NPS Buoy and climatology scatter plot and time series comparisons for air-sea temperature difference (Tsea).	37
Figure 21.	5 April to 13 May 2000 NPS Buoy and climatology scatter plot and time series comparisons for relative humidity (Rel Humidity).....	37
Figure 22.	5 April to 13 May 2000 NPS Buoy and climatology scatter plot and time series comparisons for evaporation duct height (EDH).	38
Figure 23.	5 April to 13 May 2000 NPS Buoy (blue) and COAMPS® (red) time series comparisons for air temperature (Tair), SST (Tsea), Wind Direction (WD) and Pressure (PR).	39
Figure 24.	5 April to 13 May 2000 NPS Buoy (blue) and COAMPS® (red) time series comparisons for evaporation duct height (EDH), ASTD (Tair-Tsea IR), wind speed (WS) and relative humidity (RH).	40
Figure 25.	5 April to 13 May 2000 NPS Buoy and COAMPS® scatter plot and time series comparisons for air temperature (Tair).	41
Figure 26.	5 April to 13 May 2000 NPS Buoy and COAMPS® scatter slot and time series comparisons for SST (Tsea).	41
Figure 27.	5 April to 13 May 2000 NPS Buoy and COAMPS® scatter plot and time series comparisons for relative humidity (Rel Humidity).....	42
Figure 28.	5 April to 13 May 2000 NPS Buoy and COAMPS® scatter plot and time series comparisons for air-sea temperature difference.	43
Figure 29.	5 April to 13 May 2000 NPS Buoy and COAMPS® scatter plot and time series comparisons for evaporation duct height (EDH).	43
Figure 30.	0015UTC 11 May 2000 Infrared Imagery	45
Figure 31.	0715UTC 11 May 2000 Infrared Imagery	46
Figure 32.	10-11 May 2000 NPS Buoy (blue) and COAMPS® (red) time series comparisons for air temperature (Tair), SST (Tsea), wind direction (WD) and pressure (PR).	48
Figure 33.	10-11 May 2000 NPS Buoy (blue) and COAMPS® (red) time series comparisons for evaporation duct height (EDH), ASTD (Tair-Tsea IR), wind speed (WS) and relative humidity (RH).	49
Figure 34.	0000UTC 11 May 2000 Modified Refractivity (M) with Height	50
Figure 35.	0700UTC 11 May 2000 Modified Refractivity (M) with Height	51
Figure 36.	6 April to 13 May 2000 NPS Buoy (blue) and COAMPS® (red) time series comparisons for propagation loss (PL), evaporative duct height (EDH), relative humidity (RH) and air-sea temperature difference (ASTD). Black arrows indicate 0000UTC and Green arrows indicate 0700UTC.	53
Figure 37.	0000UTC 11 May 2000 Propagation Loss Comparison, six feet above sea level (ASL), for NPS Buoy (blue), COAMPS® (red) and standard atmosphere (black).	54
Figure 38.	0700UTC 11 May 2000 Propagation Loss Comparison, six feet above sea level (ASL), for NPS Buoy (blue), COAMPS® (red) and standard atmosphere (black).	55

LIST OF TABLES

Table 1.	Flux Buoy Mean Measurement System.....	25
Table 2.	Flux Buoy Turbulent Measurement System.	26
Table 3.	Statistic summary of METOC parameters with “truth” data.	44
Table 4.	Comparison of accuracy values from different published guidelines appear in three separate columns on the LHS. Recommendations on accuracy and sensitivity for above listed data are provided in the RHS columns, from Davidson and Frederickson 2006.....	56

THIS PAGE INTENTIONALLY LEFT BLANK

EXECUTIVE SUMMARY

Commander Naval Meteorology and Oceanography Command (CNMOC) has placed emphasis on “Getting the Atmosphere and Ocean Right.” At the base of CNMOC’s three-tiered Battlespace on Demand design is the initial field for input of meteorology and oceanography (METOC) parameters. The Naval Postgraduate School (NPS) plays a key role in developing skill in this area. The first part of this study is an analysis of METOC data collected off the East Coast of the United States at Wallops Island, VA. The second part is a description of data and procedures applied in a “Proof of Concept” for a Radar Performance Surface developed and executed at NPS for the Pacific Fleet exercise Valiant Shield 2007. In both field experiments, NPS employed METOC measuring instruments and personnel in theater to collect “truth” i.e. in situ measured data to rightfully capture the “true ocean and atmosphere.”

The Radar Performance Surface reflects electromagnetic propagation reliant on the meteorological and oceanographic variability. The validity of the performance surface is a by-product of the input data. Addressed are atmospheric measurement techniques, use of climatology, and numerical modeling as the input to the Radar Performance Surface. Questions raised are: a) “How closely can we capture the true atmospheric conditions?” b) “How close are numerical models or climatology to ‘truth’ data?”

THIS PAGE INTENTIONALLY LEFT BLANK

ACKNOWLEDGMENTS

I offer my thanks and appreciation to those persons who extended their professional expertise, assistance, time and patience to the production of this thesis. My genuine appreciation is given to Kenneth Davidson, Peter Guest, Mary Jordan, Paul Frederickson and Tamar Neta.

THIS PAGE INTENTIONALLY LEFT BLANK

I. INTRODUCTION

A. MOTIVATION

This study addresses the support of non-acoustic Anti-submarine Warfare operations by timely atmospheric and ocean surface descriptions on features that impact radar and electro-optical (EO) sensor system performance. This description of lower atmosphere and surface impact on EM/EO wave propagation is critical to non-acoustic ASW operations during both the mission planning (24 to 48 hours in advance) and mission execution phases. This support should also be in line with the current NAVOCEAN Environmental Recon CONOPS by merging in situ measurements, coupled atmosphere/ocean mesoscale model forecasts and satellite-derived information to support tactical sensor systems.

The motivation for this study was to provide a “proof of concept” for a Radar Performance Surface to describe near-surface gradient impact on submarine periscope detection. Radar detection was identified as a current concern with regard to transitioning present and near-future operational meteorology and oceanography (METOC) products. Electro-optical detection displays will most likely follow the radar-based Performance Surface development.

CNMOC’s Battlespace On Demand (BOND) is the overarching framework that guides and informs the efforts of the U.S. Naval Oceanography Program with the Naval Maritime Strategy and the Navy’s Operations Concept. It provides the course to vertically align and inform Navy’s programmatic investments in Naval Oceanography, from science and technology, through research and development, and transition to operations. It provides a systematic approach to convert knowledge of today’s oceanographic environment into tomorrow’s warfighting efforts. Figure 1 displays the three-tier framework for Naval Oceanography.

Battlespace on Demand

The Three Tiers

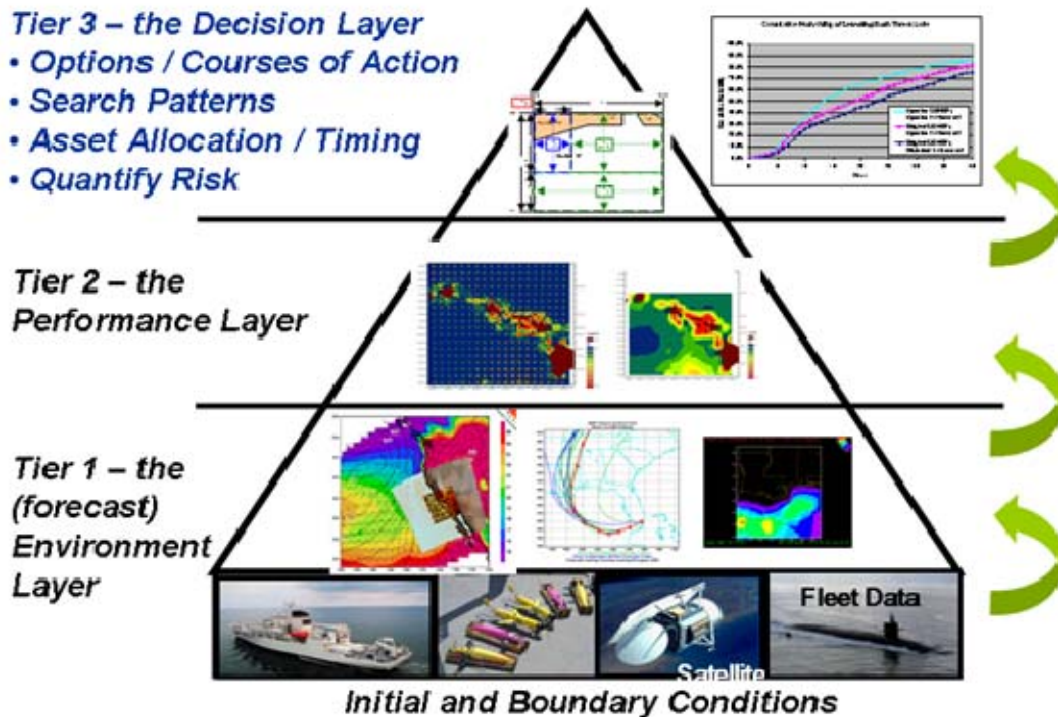


Figure 1. CNMOC Battlespace on Demand. CONOPS for Naval Oceanography

The atmospheric and ocean surface descriptions, which reside in tier 1 of the “BOND Pyramid,” need to be applied to radar performance models that predict the effects of the near-surface gradients of refractivity, i.e., gradients that lead to normal, sub-refractive, or trapping conditions. Trapping conditions immediately above the surface are responsible for what is called the evaporation duct. Sub-refraction leads to reduced ranges, while trapping or evaporative ducting leads to increased range but also increased clutter. Near-surface refraction has a major impact on the performance of surface platform radar systems. This study is based on results from both field tests and operational (fleet exercise) events, Wallops Island 2000 and Valiant Shield 2007.

B. APPLICATION

The Radar Performance Surface is a contoured display of range describing the near-surface refractivity impact on radar systems for submarine periscope detection with a probability of detection (POD) of 90%. This display is the application for the “Proof of Concept” development of a Radar Performance Surface for operational METOC and ASW CONOPS. The development accounts for various data input, effects modeling, merging of detection thresholds for a display of detection impact. The propagation and effects model applications occur in tier 2 of the BOND Pyramid. This performance surface will be produced for varying properties of the near-surface airflow and surface conditions. The demonstration is based on data collection and conditions that occurred during two separate field campaigns with one being an experiment-based field test for radar performance estimation (Wallops 2000), and the other being a Fleet Battle Experiment (Valiant Shield 2007).

The “Proof of Concept” Radar Performance Surface presented in this study was formed with the integration of data sources to relate to refraction and propagation. Effects models are used describe the propagation and its impact on radar sensor’s performance. Figure 2 shows the components of six-step integration with respect to data sources. The four input data sources are platform in situ, mesoscale model, and climatology. In Chapter II, Background, airflow parameters will be related to near-surface refractivity, and lead to impacting conditions, super-refractive, trapping and evaporation duct, and sub-refractive layers. A method to relate operational or bulk parameters to the refractivity will be presented. In situ measurements of these bulk parameters are the “truth” with regard to data sources. Chapter II will also present significant aspects of three of the data sources: Climatology data, COAMPS[®] predictions and Satellite data.

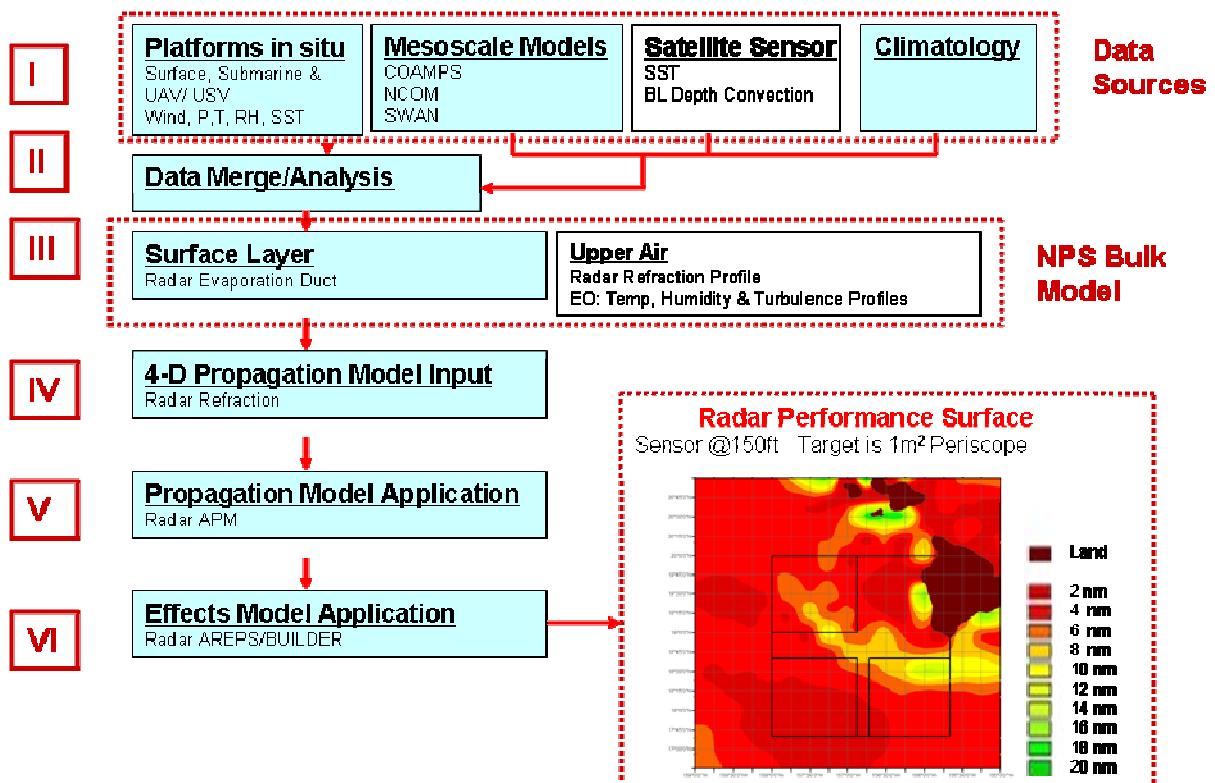


Figure 2. Integrated Approach for Data Source

II. BACKGROUND

A. ATMOSPHERE CONDITIONS AND REFRACTION

1. Introduction

Results derived in this study are based on special analyses of procedures and data applied in two field campaigns that were conducted for different reasons. In one, radar performance had a central role since it was designed with respect to making radar setting adjustments for atmosphere conditions. This will be referred to as the “Wallops Island 2000 Field Experiment”. The second was the Naval ASW Fleet Exercise Valiant Shield in 2007 (VS07). VS07 focused primarily on collecting near-surface air-flow and surface temperature measurements to make direct comparisons to the Coupled Ocean Atmosphere Mesoscale Prediction System (COAMPS®) as a prime source of input to the Radar Performance Surface. This was also an opportunity to examine the Navy’s existing methods for collecting near-surface air-flow and surface temperatures.

Both of these field campaigns yielded data sets, EM sensor performance measures, and scenarios that enabled performance and evaluation of components within the “Proof of Concept” for the Performance surface. This was because the “Proof of Concept” focused on the near-surface EM refraction gradients as the impact on radar sensor’s performance. For this purpose, the field campaigns were supported with data collection of lower atmosphere and ocean surface conditions by the Department of Meteorology of the Naval Postgraduate School (NPS/MR) Monterey, California, and by mesoscale model predictions of lower atmosphere conditions performed by the Marine Meteorology Division of the Naval Research Laboratory, Monterey (NRL-MM/MRY). The mesoscale model system used was COAMPS®. The propagation and effects models applied to the “truth” and COAMPS® data sets were those developed by Space and Naval Warfare Systems Center, San Diego (SSC-SD). The propagation model was the SSC Advanced Propagation Model (APM). Both NRL/MRY and SSC-SD are listed as partners in the integrated approach to Performance Surface development, displayed in Figure 2.

In the following subsections, impacting refractive conditions are presented and estimations of them are described.

2. Refractivity

Temporal and specially varying near-surface meteorological and ocean surface features are known to affect electromagnetic (EM) propagation. Over the sea, either large negative (trapping) or positive (sub-refractive) gradients of refractivity have the greatest effect on radar and communications systems performance. These conditions yield greater horizontal (trapping) or significantly reduced (sub-refraction) ranges over the earth's surface.

The bending of EM rays is called refraction. All propagation of EM rays in the atmosphere refract to some degree. An electromagnetic ray describes the wave-front propagation direction and is normal to the wave-front. Refraction modifies the direction of propagation of a wave-front. Refraction is controlled by the index of refraction, (n) which is defined by the ratio of wave speed in free space (c) to wave speed in the medium (v), equation 1. EM rays bend toward regions of slower wave propagation speeds or higher n . Gradients of n with height across the propagation path cause refraction or curvature of the EM ray.

Because values of n are nearly equal to unity, a more conventional use of n is used in equation 2 to derive the term Refractivity Index (N). Applicable to microwave frequencies and below, N is calculated in equation 3 ([Bean and Dutton, 1968](#)) using atmospheric parameters of absolute temperature (T), partial pressure of water vapor (e) and atmospheric pressure (P) where T is in degrees Kelvin, and P and e are in millibars (mb).

$$n = \frac{c}{v} \tag{Eqn 1}$$

$$N = (n - 1) \times 10^6 \quad \text{Eqn 2}$$

$$N = 77.6 \frac{P}{T} - 5.6 \frac{e}{T} + 3.73 \times 10^5 \frac{e}{T^2} \quad \text{Eqn 3}$$

To account for the earth's curvature as EM energy travels in its atmosphere, N is corrected or modified for the curvature gradient of approximately -0.1568m^{-1} . The Modified Refractivity Index (M) is expressed in equation 4, where (r_e) is the earth's radius ($6.378 \times 10^6\text{m}$) and (z) is the height above the surface in meters.

$$M = N + \frac{z}{r_e \times 10^{-6}} = N + 0.1568z \quad \text{Eqn 4}$$

The vertical gradients of N or M (dN/dz or dM/dz) define the four general refractive categories of ducting (trapping), normal, super and sub-refraction shown in Figure 3. Radar propagation with respect to the horizon is best described by the vertical gradient of refractivity N (dN/dz) and with respect to the earth's surface by the vertical gradient of M (dM/dz). When dN/dz is greater than zero, rays turn upward relative to the earth's surface. When dM/dz equal zero, the EM ray curvature is equal to the earth's curvature.

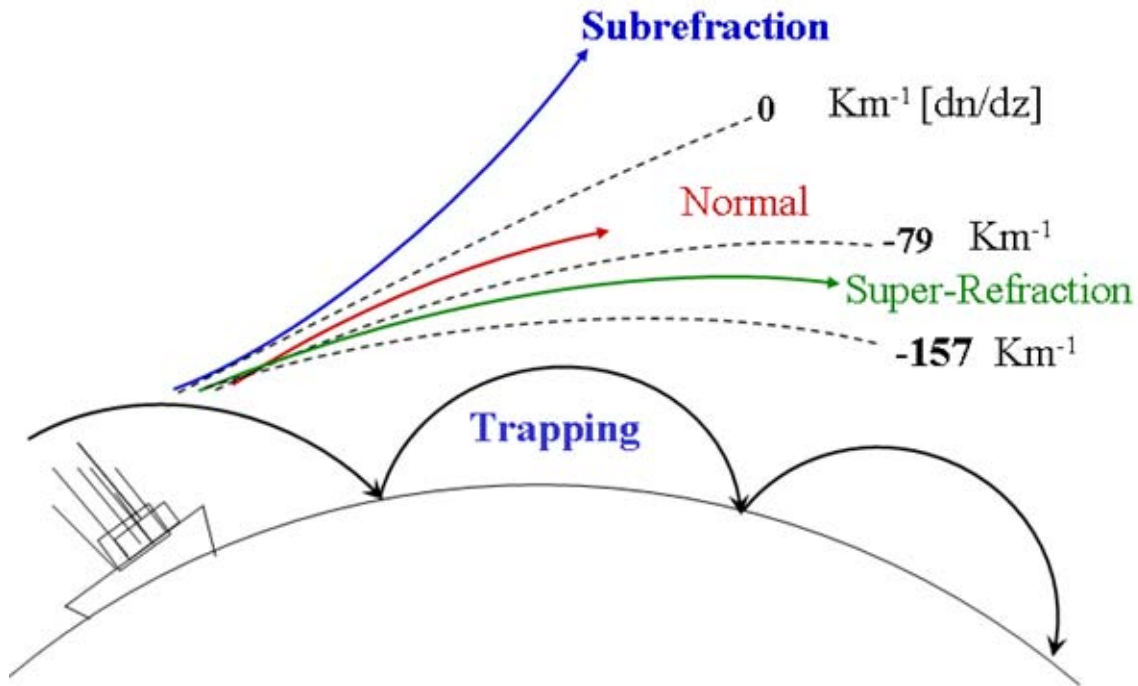


Figure 3. Refraction Categories.

3. Super-Refraction

Super-refraction requires a decrease in modified refractivity with height at a rate greater than the standard atmosphere. Trapping or super-refraction can occur with any one or combination of the following conditions:

- A large *increase* in temperature with height.
- A decrease of specific humidity or other measure of moisture content with height.

4. Trapping Layer and the Evaporation Duct

The evaporation duct is the name given to a trapping layers caused by the humidity gradient, immediately over the sea. It is shown by the gradient of the Modified

Refractive Index (M) with height. A standard atmosphere leading to typical profiles of M and (refractivity index) N are illustrated in Figure 4.

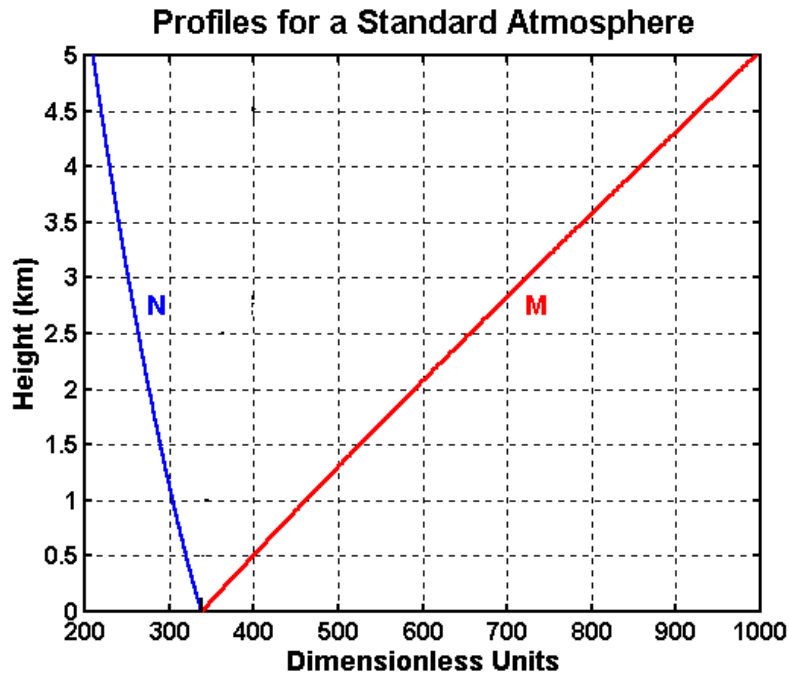


Figure 4. Profiles for a Standard Atmosphere

A trapping layer is characterized by a large negative refractive gradient and normally requires the air temperature to increase and humidity to decrease with height. However, the humidity gradient is the most critical determinant. Formation of typical ducting conditions are associated with dry air overlying relatively moist air and enhanced by the overlying air being warmer. Oceanic environments experience a widespread and persistent evaporative duct due to their saturated moist surfaces.

The top of the trapping layer, where dM/dz equal zero, is referred to as the Evaporation Duct Height (EDH). Since dM/dz is less than zero below this level, it is the first level of the minimum value of M above the surface. At the EDH, the gradient of M is zero and represents the boundary where the wave-guide would refract upward or refract

downward toward the earth surface. Evaporative ducting affects signals greater than 2 GHz. Figure 5 displays this minimum value of M as the EDH. Propagation just above, although not trapped, will cause extended propagation ranges as well.

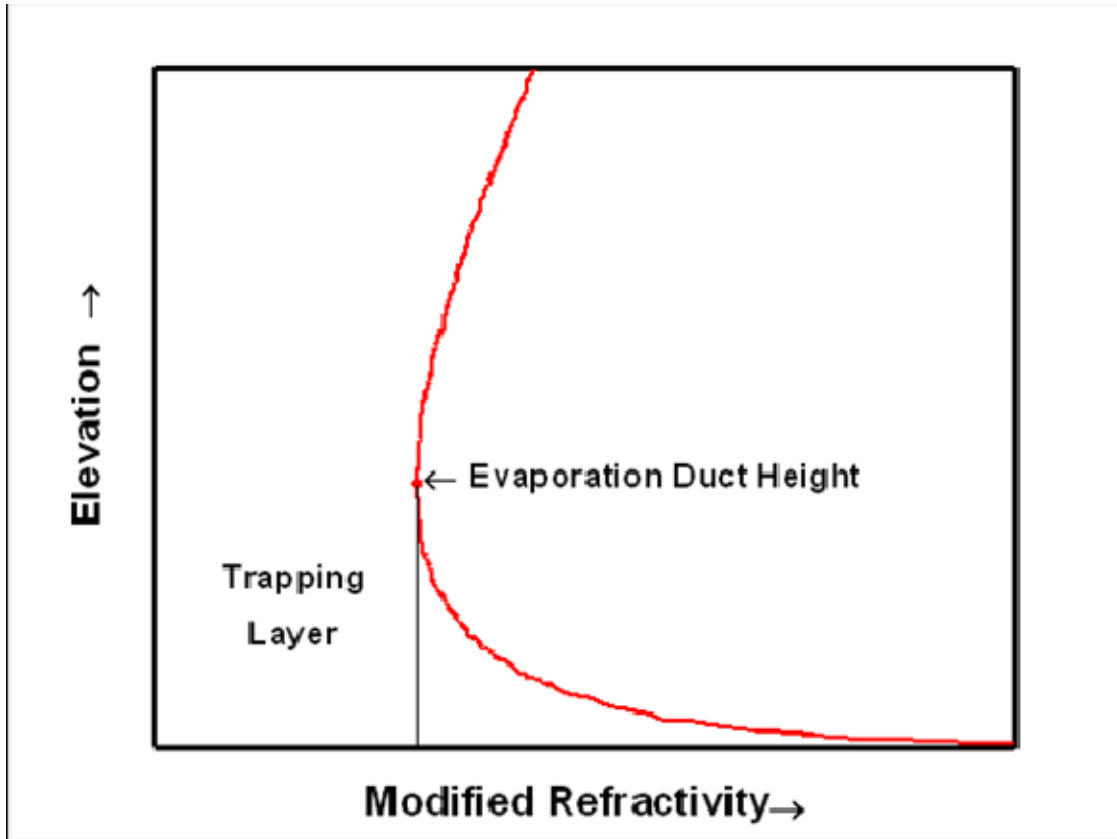


Figure 5. Plot of a typical vertical modified refractivity profile with corresponding evaporation duct height and trapping layer. From: ([Frederickson et al., 2000b](#)).

As a result of the evaporation duct, or wave guide, EM energy could propagate over the ocean surface at greater than normal distances. If an evaporation duct is present, military platforms' sensor and communication systems have the potential advantage of exploiting such meteorological phenomena to gain greater ranges for detection over the horizon. For this and other applicable reasons, it is imperative to properly describe the presence of such ducting.

The Air Sea Temperature Difference (ASTD) determines to the stability of the lower atmosphere where a greater (lower) sea surface temperature leads to negative (positive) stability. Therefore, the ASTD controls the shape of the M profile due to its influence on mixing. A consideration for study is that in certain meteorological situation e.g. frontal passage or strong diurnal effects where surface temperature gradients vary significantly on short time scales, numerical mesoscale models may fail to capture the proper ASTD. This would lead to improper representation of the near-surface refractivity profile or the evaporation duct. Typically, an unstable stable lower overwater layer leads to an EDH and trapping conditions. In stable conditions other factor must be considered for predicting trapping. However with the airflow nearly 100%, or near saturation, a stable low lower overwater layer has the likelihood of sub-refraction since increase of temperature with height would imply an increase of vapor pressure with height.

5. Sub-refraction

Sub-refraction is caused by an increase in modified refractivity with height at a rate greater than the standard atmosphere. Sub-refraction can occur in either of the following conditions:

- A lapse rate of temperature *greater* than standard or a decrease in temperature with height.
- A lapse rate of relative humidity gradient *less* than standard, or an *increase* in moisture content with height.

The evaporation duct is caused by the gradient of the Modified Refractive Index (M) with height. The shape of a M profile gives further indication of ducting, super and sub-refractive conditions. A warmer ocean surface than the air directly above it will produce an unstable condition while a colder underlying ocean surface than the air above it will produce a stable lower atmosphere.

B. REFRACTIVITY FROM BULK SURFACE LAYER MODELS

Operational estimates of the near-surface refractivity require application of models that would allow the gradients description from what are referred as “bulk” data, thus the term “bulk models”. Bulk data are near-surface mean values of wind speed, wind direction, pressure, and air and sea temperature. Direct measurements of the evaporation duct require multi-level fixed sensors or moveable sensors such as tethered balloons or kites starting near the surface and extending to heights above the EDH. Such an approach is unpractical for most operational situations. The typical evaporation duct height range is from two to fifty meters. Typically naval ships mean measurements (wind speed, temperature, humidity and pressure) are available at some reference height. Sea Surface Temperature (SST) is normally obtained continuously by a sea water intake or manually by METOC personnel via hand held infrared gun. IR measurements are a directed and/or mandated measuring tool and their use on Aircraft Carriers are inconsistent through out the Naval Fleet.

Monin-Obukhov Similarity (MOS) theory establishes the approach for the models. According to strict MOS theory, conditions are assumed to be horizontally homogeneous and stationary. The turbulent fluxes of momentum, sensible heat and latent heat are assumed to be constant with height in the surface layer. The surface layer is the lowest 10% of the turbulent atmospheric boundary layer, and generally extends upward to a height of roughly ten to two hundred meters. However, MOS theory has been shown to be valid even when these conditions are not strictly met so this approach is applicable to most situations over the ocean.

Bulk models for the surface-layer, based on MOS theory, are what allow the use of mean single-height measurements in conjunction with value for the SST to estimate the temperature and humidity surface-layer profiles that are needed to calculate near-surface refractivity profiles. The refractivity profile is then interpreted for the presence and height of evaporation ducts. Empirically formulated models that use the MOS theory

to relate profiles to surface fluxes use bulk measurements at a single level in the atmosphere and the surface (Fairall et al., 1996).

This thesis uses the Naval Postgraduate School (NPS) model which is based on the LKB (Liu et al., 1979 and Fairall et al., 1996) bulk surface-layer scaling model ([Frederickson et al., 2000a](#)) within the MOS approach to determine the near-surface modified refractivity (M) profile. The NPS model is also similar to a version described by [Babin et al. \(1997\)](#), which was formulated directly from the LKB, and is a recent model for the evaporation duct. There are several important differences between the NPS model and that described by [Babin et al.](#) For example, the NPS model's integrated profile functions for stable conditions are different than the Businger-Dyer type functions used by [Babin et al.](#) The use of the new functions result in convergence of the model solution in many highly stable, low wind speed conditions in which the Businger-Dyer functions would result in non-convergence. The model also uses a new form for the thermal roughness Reynolds number R_θ , which unlike the discrete original LKB functions, has no first order discontinuities and is also much simpler to implement.

The NPS approach computes the N or M profiles and determines impact on propagation. Babin et al. used an iterative method to determine the evaporation duct height. Both approaches provide operational users with other useful EM propagation information such as the shape of the near-surface profile and the occurrence of sub-refraction.

The NPS model is based on the full definition for refractivity (N) including both vapor pressure terms in the right hand term of equation three. While this term is generally small, in certain stable conditions it can modify the vertical N profile enough to significantly change the evaporation duct height ([Frederickson et al., 2000b](#)). Finally, the NPS methodology includes operational checks for valid input data ranges and indicates no solution is possible when the data are outside the valid ranges. This avoids the possibility of the operator receiving an erroneous model solution based on obviously bad input data.

The bulk model enables one to examine the sensitivity of the evaporation duct height to stability. This sensitivity is represented in Figures 6-8, where the EDH is calculated by NPS bulk model. The EDH is calculated with respect to the ASTD for 12°C for three wind speeds (2, 5 and 10 ms⁻¹). Further, they show the impact of four different relative humidities of 40, 60, 80 and 100%.

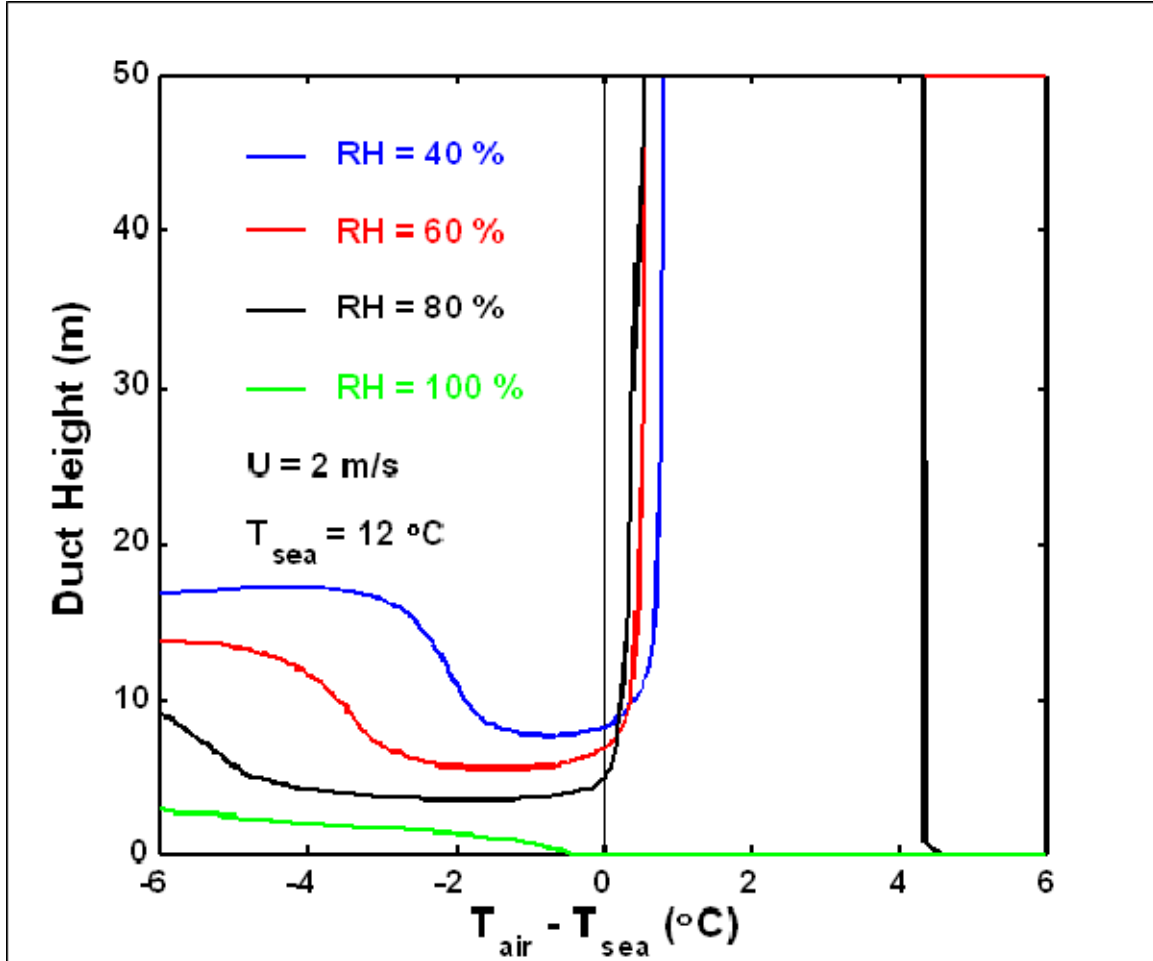


Figure 6. Plot of model computed evaporation duct heights versus model input air – sea temperature differences, computed with wind speed (U) = 2 m/s, T_{sea} = 12 °C and different values of relative humidity as indicated. From: ([Frederickson, 2000b](#)).

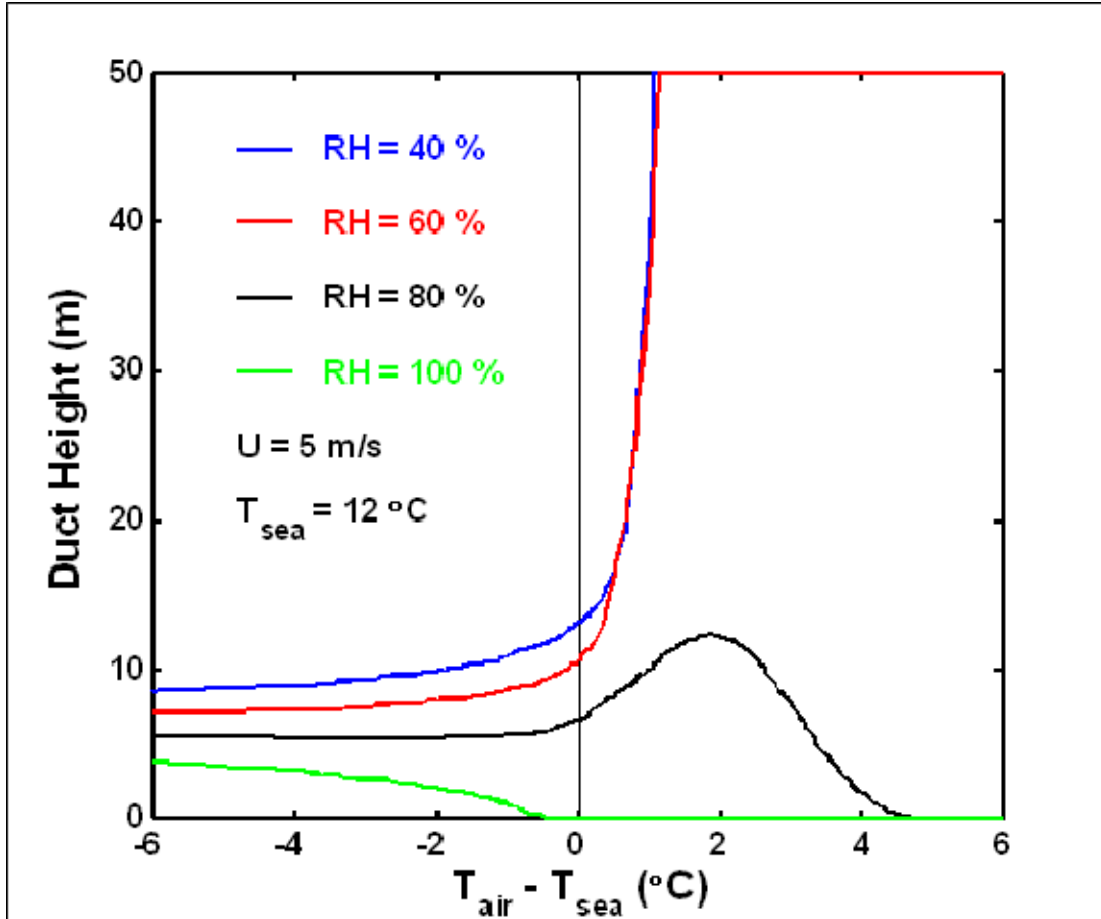


Figure 7. Plot of model computed evaporation duct heights versus model input air – sea temperature differences, computed with wind speed (U) = 5 m/s, $T_{\text{sea}} = 12 \text{ °C}$ and different values of relative humidity as indicated. From: ([Frederickson, 2000b](#)).

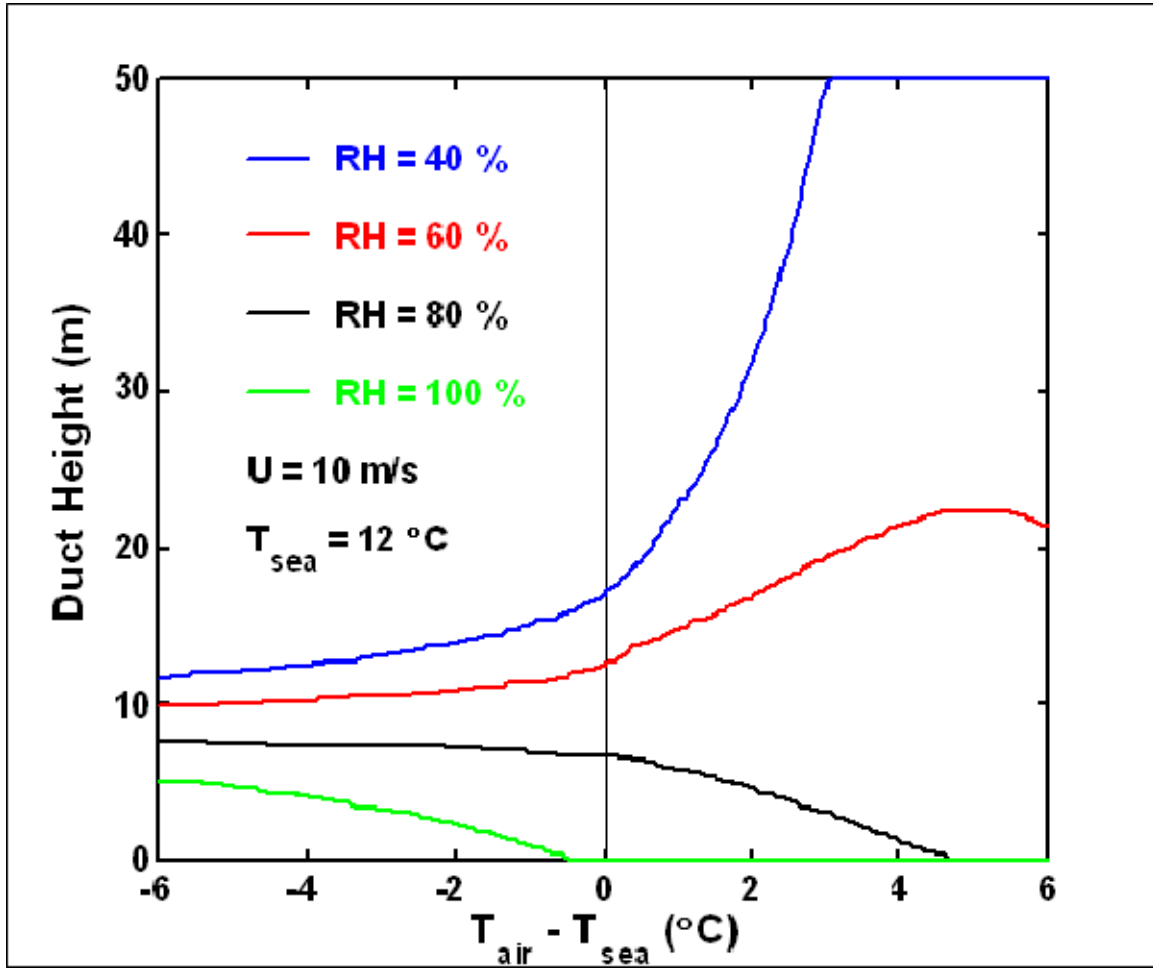


Figure 8. Plot of model computed evaporation duct heights versus model input air – sea temperature differences, computed with wind speed (U) = 10 m/s, T_{sea} = 12 °C and different values of relative humidity as indicated. From: ([Frederickson, 2000b](#)).

Climatology data were archived from the National Climate Data Center’s NCEP-DOE Reanalysis 2 Gaussian Grid with a temporal coverage of 4-times daily values from 1 January 1979 to present. Spatially, the Global T62 Gaussian grid (192x94) was utilized with the closest grid point to the NPS Buoy displayed in Figure 9. Climatology was utilized to make legitimate comparisons of “truth” data with archived long term means of METOC parameters. The reanalysis data were collected four times (0000, 0600, 1200

and 1800UTC) daily for each day during to appropriate Wallops Island 2000 data. Plotted time series of climatology with NPS Flux Buoy are presented in the results.

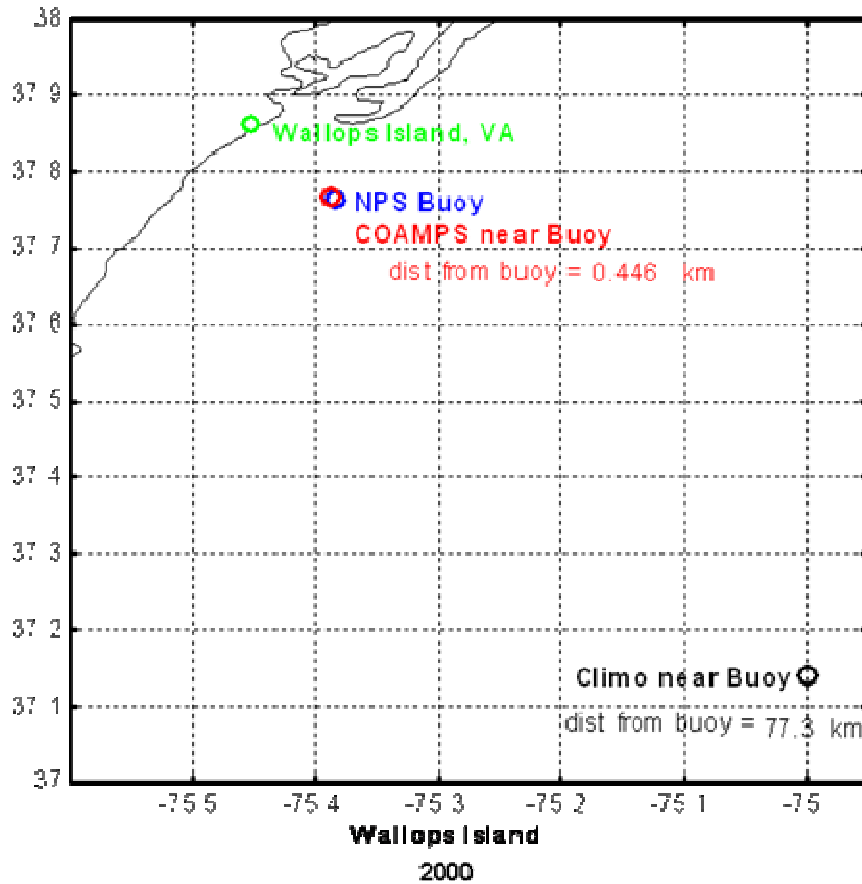


Figure 9. Spatial display of NPS Buoy, COAMPS® and Climatology grid points.

C. HIGH RESOLUTION COAMPS®

A Numerical Weather Prediction (NWP) system was employed in this thesis to evaluate application of such a model to provide the determining bulk parameters. The NWP system employed was the Navy's Coupled Ocean Atmosphere Mesoscale Prediction System (COAMPS®). Values from COAMPS® three kilometer resolution model were compared to those from the NPS Flux Buoy. COAMPS® provides a 4D

NWP, with 3D being predictions at grid-points with varying horizontal and vertical distances, and the fourth dimension being time, out to 48 hours. In this study, the in situ collected data are assumed to be “truth” which are compared to values of COAMPS[®] fields.

The Marine Meteorology Division of the Naval Research Laboratory COAMPS[®] uses the non-hydrostatic, fully compressible equations of motion for the atmosphere. Prognostic equations in COAMPS[®] include those that account for the atmosphere parameters impacting refraction, and hence EM propagation. Those of concern are wind, pressure, temperature, and water vapor. In the COAMPS[®] model, the parameterizations are utilized for surface and boundary layer processes, radiation, moist physics and convection.

COAMPS[®] has two components for atmospheric projections: analysis and forecast. Unlike forecasting, the analysis or initial field is generated from multiple data sources. Global forecasts from the Navy Operational Global Atmospheric Prediction System (NOGAPS) are utilized by COAMPS[®] for boundary conditions. Initial field data in COAMPS[®] are gathered from observed data from satellites sensors, aircraft measurements, surface and upper-air land stations, buoys or ships' observations along with previous model 12-hour forecasts. The input data in all cases depend on availability of observations at the time the analyses performed.

Key for this study's COAMPS[®] application is that horizontal and vertical spatial resolutions are high enough to describe most features that are important to refraction effects. Available COAMPS[®] data used in Wallops Island 2000 were nested grids with three different grid resolutions centered off the Eastern Shore of Virginia, in the vicinity of Wallops Island, VA. The three horizontal grid resolutions are 3, 6, and 18 km, with 3 km with Wallops Island within the 3 km grid. COAMPS[®] calculates a vertical profile by both analyzing and forecasting variables at pressure levels assigned on the basis of fractional differences from the surface pressure, i.e. sigma levels. Normal vertical spacing with the high-resolution COAMPS[®] yields parameter values at 5, 15, 25, 35, 45, 55, 67.5,

85 and 105 meters. Hence, surface-layer values are predicted that can be used with the NPS bulk model to calculate the evaporation duct profile, at higher resolutions.

COAMPS[®] predictions provide hourly fields of atmosphere parameters from 12-hour forecasts initiated at 0000 UTC for the days 5 April to 13 May 2000. Two runs are performed at 0000UTC and 1200UTC for each day of interest. The sea surface temperature (SST) field is held constant for each 12-hour forecast.

For the bulk methods, the only environmental input parameters needed are sea surface temperature, and air temperature, wind speed, relative humidity, and pressure at a known height. The lowest sigma level of the COAMPS[®] were used (which has a height of 5 meters) was used because the model produces u and v wind components, potential temperature, water vapor, and pressure fields at the sigma levels hourly. This level is virtually always in the surface layer and the MOS theory is applicable. The sea surface temperature field in COAMPS[®] is constant for each model run. The air surface interaction in COAMPS[®], as used for this study, was based on the Louis (1979) surface layer parameterization scheme (Hodur, 1996). In this scheme polynomial functions of the bulk Richardson number are used to directly compute the surface fluxes. The surface fluxes boundary conditions establish mean values in the lower levels.

The COAMPS[®] option for the surface layer parameterization based on the TOGA-COARE scheme (Fairall et al., 1996) was not available for this study. This is important to note because it forms the basis of the NPS bulk model, which was used to calculate the profiles that were then applied to APM. The TOGA-COARE scheme differs from the scheme used in older versions of COAMPS[®] by

- different functional forms for z_{0t} and z_{0q}
- Uses similarity theory directly
- Has polynomial approximation for stability function on the unstable side

D. SATELLITE DATA

Data obtained from satellite borne sensors are important to refractivity condition assessment by COAMPS[®] initialization and are used to identify an influencing weather system. Satellite sensor derived SST, from IR signatures, are the primary source used to initialize COAMPS[®]. Satellite images provide evidence of frontal systems and passages, hence air-mass property changes, and convective cloud mixing processes that disrupt upper level refractive layers. Further, satellite multi-spectral sensor data can be used to yield operational quantitative information on upper level trapping layers for stratus (non-convective) cloud occurrences (McBride, 2000).

E. PROPAGATION EFFECTS MODEL APPLICATION, APM

The integrated approach for the Radar Performance Surface, shown in Figure 2, requires an effects model to describe the influence of atmosphere on propagation. As such, the propagation and effects model are those components that reside in tier 2 of the “Battlespace on Demand” pyramid, Figure 1. Advanced Propagation Model (APM) is applied in this study. The Advanced Refractive Effects Prediction System (AREPS) is a “shell” that uses the APM for calculation of EM propagation. Both models were developed by the Space and Naval Warfare Systems Center, San Diego (SPAWAR). AREPS features a Graphics User Interface (GUI) that allows the user to input environmental and radar system information into the APM for generating two-dimensional views of propagation loss, vertical M-profiles, and propagation condition summaries from model calculations.

AREPS has incorporated the NPS evaporation duct model for computing near-surface M profiles from specified input parameters. This study uses APM and is valid for the following frequency ranges: 100 MHz to 20 GHz. It is a combination of the Radio Physical Optics (RPO) model and the Terrain Parabolic Equation Model (TPEM). APM models propagation impacts of pre-loaded 2-D and 3-D radars and uses imported environmental data. The ability to import specific data from in situ measurements, such

as bulk in situ surface and surface-layer measurements, launched radiosonde profiles, or from model predictions, such as COAMPS[®] is supported.

APM uses the Parabolic Equation (PE) algorithm for propagation loss under a maximum propagation angle, which will then dictate the maximum ranges and heights. Figure 10 shows the different regions in the APM. In this study, the application region for APM was the PE region since the radar and target were assumed to be in the surface layer, over the sea. In APM, propagation loss is calculated for other predetermined zones using three other algorithms. The algorithms are the flat earth (FE), the ray optics (RO), and the extended optics (XO). The elevation angle based predetermined regions and other aspects of APM are described by Hitney 1994.

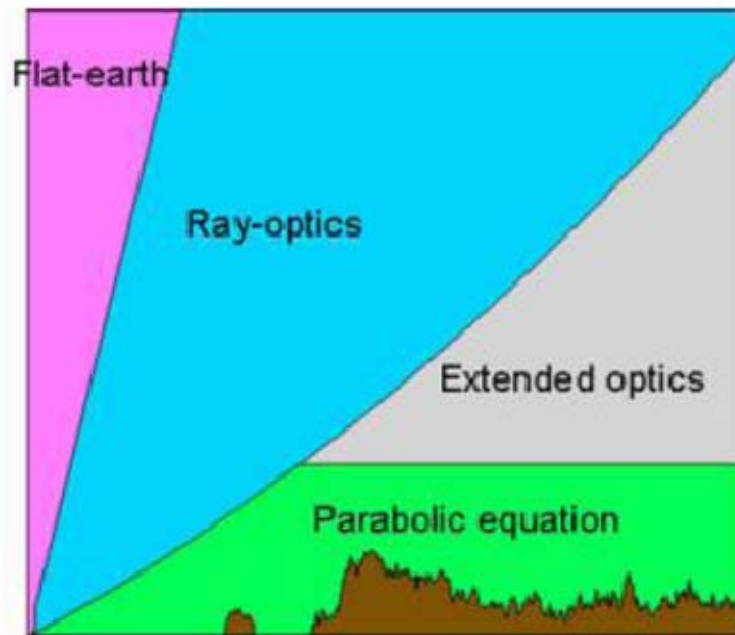


Figure 10. Propagation regions in the Advanced Propagation Model (Hitney, H. V., 1994)

THIS PAGE INTENTIONALLY LEFT BLANK

III. WALLOPS ISLAND 2000 FIELD EXPERIMENT

A. INTRODUCTION

In April and May of 2000, personnel from the Theater Warfare Systems Department of the Navy's Surface Warfare Center, Dahlgren, VA (NSWC-DD) conducted a series of radio frequency (RF) tests and experiments at the Navy's Surface Combat Systems Center, (SCSC) Wallops Island, VA. The tests supported the "Interactive Adaptation of Fire Control Sensors to the Environment" task by collecting pertinent data in environments encountered by ships at sea. The principal objective of the experiments was to develop methods by which ships could remotely sense low altitude propagation and clutter using ship-borne fire control sensors and local meteorological measurements.

The tests also included: a) evaluating the degree of which mesoscale models can accurately predict the true predicted propagation conditions based on comparisons with in situ data, b) direct EM measurements that can be used to validate propagation models and c) evaluating METOC collection techniques.

1. Purpose

The METOC parameters collected by personnel at NPS's Department of Meteorology at Wallops Island allowed estimations of the sensitivity of near-surface refractive conditions to the air flow properties, e.g., humidity or fluctuations in stability. It is believed that subtle stability fluctuations cause significant changes in refraction conditions to either bring about extended EM propagation or the lack thereof. For this purpose, COAMPS[®] predictions were compared to the Wallops Island in situ collected data referred to as "truth". This will be used to point out inefficiencies in model predictions for the Radar Performance Surface to capture short temporal meteorological mesoscale changes in the boundary layer. Previous studies have shown COAMPS[®] has

difficulties in capturing small scale and rapidly changing atmospheric conditions. The ultimate goal of the comparison is to initiate model upgrades.

2. Naval Postgraduate School Flux Buoy

Personnel from the Department of Meteorology, NPS deployed a flux buoy in the Wallops Island 2000 for the entire campaign (Figure 11). The data collection period extended from the 1 April through mid-June 2000. The buoy was moored seven nautical miles off shore at: $37^{\circ} 45.8' \text{ N}$, $75^{\circ} 23.1' \text{ W}$ in a region of mean depth of approximately fourteen meters (Figure 9).

The flux buoy provided data of high frequency atmospheric turbulence, mean meteorological fields, sea temperature, platform motion data and wave spectra data for this entire period. The flux buoy is a two meter diameter disk buoy instrumented with sensors to measure mean and turbulent airflow parameters, SST and two-dimensional wave spectra.



Figure 11. NPS Flux Buoy

B “TRUTH”/BUOY DATA COLLECTION

1. Mean Environmental and Turbulent Data Collection System

The meteorological data acquisition system sampled environmental data from a suite of instruments at 1 Hz. These 1 Hz values were averaged into one-minute blocks that were then stored in the onboard computer. The wind direction and buoy heading were unit-vector averaged to handle the jump between 360 – 0 degrees. The flux buoy mean sensors are described in Table 1.

Measured Parameters	Sensor Type	Manufacturer and Model	Height Above Surface
Wind Speed/Direction	Propeller-vane anemometer	R. M. Young Wind Monitor Model 05106	3.90 meters
Air Temperature	Pt 100 RTD	Rotronic MP101A	3.94 meters
Relative Humidity	Rotronic Hygrometer	Rotronic MP101A	3.94 meters
Atmospheric Pressure	Barometer	A.I.R.	2.10 meters
Sea Surface Temperature	IR Temperature Transducer	Everest Model 4000	2.40 meters
Bulk Sea Temperature	Hull thermistor	NPS custom design	–1.17 meters
Buoy Heading	Compass	TCM-2	0.39 m

Table 1. Flux Buoy Mean Measurement System

The buoy also measured flux turbulent parameters (Table 2). These data were stored in the onboard computer in files containing a 77-minute time series record. These flux data may be valuable for future evaluation of COAMPS® parameters. These fast sampled sensors measured three-dimensional wind speed, temperature and the buoy’s three-dimensional accelerations and angular rotations.

Measured Parameters	Sensor Type	Manufacturer and Model	Height above Surface
3-D Wind Speed & Sonic Temperature	3-D Ultrasonic anemometer	Gill Instruments Model 1210R3	5.23 meters
3-D Platform Motion	Accelerometers & Rate gyros	Crossbow DMU-VGX	0.39 meters
Buoy Heading	Magnetic compass	TCM-2	0.39 meters

Table 2. Flux Buoy Turbulent Measurement System.

C. BULK PARAMETERIZATION PROCESSING FOR WALLOPS 2000

1. The Near-Surface Layer Scaling Parameters: Profile Properties and Evaporation Duct Height

The measurements described previously provide bulk “truth” information with respect to the airflow and surface properties. It was then necessary to relate these to features that affect radar refractivity profiles, which are in tier 2 of the BOM pyramid. As such, atmospheric surface layer profiles that determine the evaporation duct and sub-refractive conditions were estimated by applying scaling expressions to mean METOC properties measured at one level in the air and the surface temperature. Mean environmental measurements were averaged into five minute blocks. All parameters were scalar averaged, with the exception of the wind direction which was vector averaged.

IV. VALIANT SHIELD 2007 “PROOF OF CONCEPT” FOR RADAR PERFORMANCE SURFACE

ASW Fleet Exercise Valiant Shield 2007 (VS07) was a large war game conducted by the United States military in the Pacific Ocean in August 2007. The exercise began on 7 August 2007 and lasted until 14 August 2007. Valiant Shield focused on cooperation between military branches and on the detection, tracking, and engagement of units at sea, in the air, and on land in response to a wide range of missions.

A. FIELD COLLECTION

The author embarked on the Research Vessel (RV) Cory Chouest for VS07 to take air flow and sea surface temperature measurements. The RV Cory Chouest is one of the fleets' Surveillance Towed Array Sensor System (SURTASS) Low Frequency Active (LFA) ships which participated in VS07. A meteorology package was built by NPS to contain an aspirated temperature and relative humidity sensor, a GPS, a wind vane (wind speed and direction) and an infrared sensor for sea surface measurements. This METOC package was fixed on the highest and most forward attainable deck on the RV Cory Chouest.

Personnel from the Department of Meteorology, NPS purchased four Infrared Radiation Pyrometers, Heitronics model KT15.82, specifically for VS07 to accurately measure the skin surface of the ocean, operating in the range of 8-14 microns (Figure 12). The infrared sensor measures the skin temperature of the sea surface which is the very top of the sea surface which is not measured by other SST sensors. A self-contained battery pack, data logger and protective housing for the highly sensitive passive infrared sensors were built by the Department of Meteorology at NPS and deployed on the RV Cory Chouest, USS Kitty Hawk, USS Nimitz and USS John C. Stennis, all participated in the VS07 exercise. The weather office onboard the USS platforms obtained a SST measurement, via the KT15.82, every hour for the full duration of VS07.

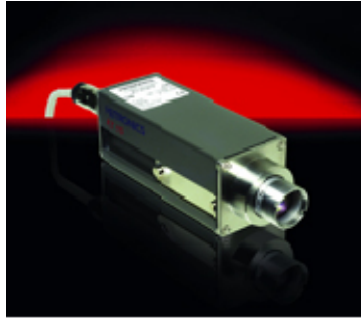


Figure 12. Infrared Radiation Pyrometers, model KT15.82, Wintronics 2007

The “truth” data collected in this field experiment and for the most part any in-situ data obtained in a field campaign are a valuable means for evaluation of sensitivities of METOC parameters as input to atmospheric performance surfaces.

B. DEVELOPMENT OF THE RADAR PERFORMANCE SURFACE

The Naval Postgraduate School developed the Radar Performance Surface as a “Proof of Concept” for the fleet exercise VS07. The Radar Performance Surface is a contoured display of range describing the near-surface refractivity impact on radar systems for submarine periscope detection with a probability of detection (POD) of 90%.

The Radar Performance Surface was produced in the Systems Technology Battle Laboratory (STBL) at NPS. Manual steps and execution time typically took one hour. A simplified flow diagram displays the methodology in formulating the display (Figure 13).

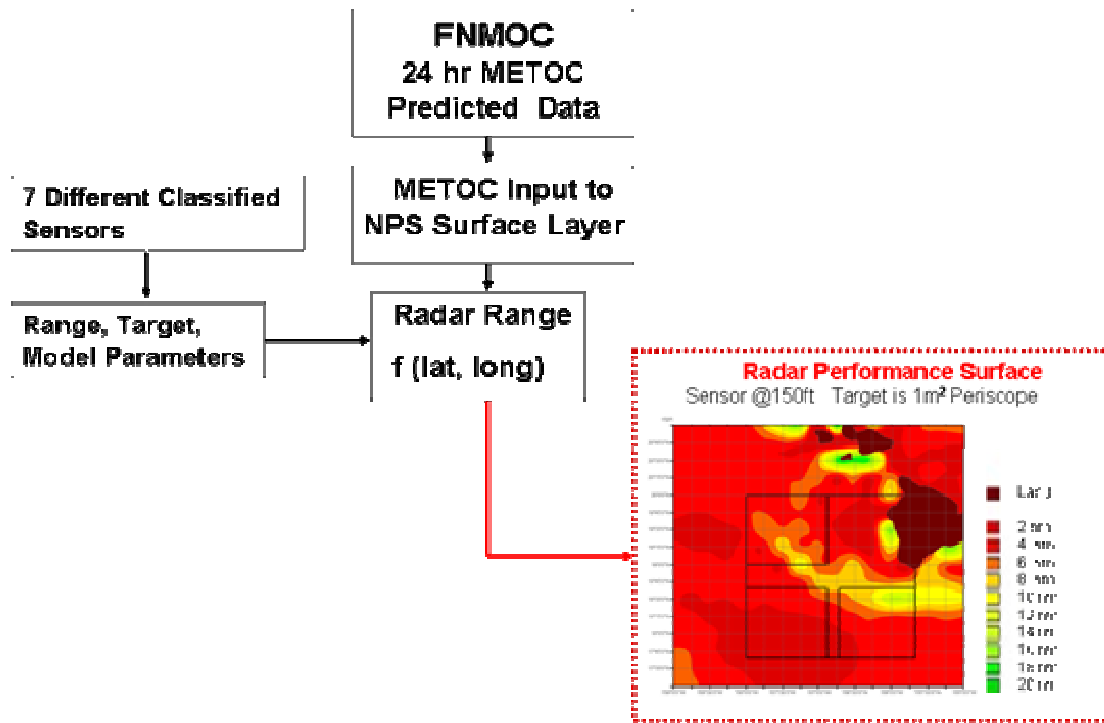


Figure 13. Flow Diagram for producing the Radar Performance Surface

The Fleet Numerical Meteorology and Oceanography Center provided COAMPS[®] fields in the form of Gridded Binary (GRIB) data files which were downloaded from the SIPRNET at NPS. The 24-hour forecasted METOC data was in the form of 10 meter wind vector, pressure, relative humidity, air and sea temperature. The NPS Surface Layer Model calculated low level profiles of specific humidity and temperature based on above inputs for the operational area. That information was used to calculate the modified refractivity, M profile for each grid point in the VS07 spatial domain. The M profile is used as an input to the APM. Output from the APM produces radar signal strength as a function of height and range for each point. A NPS Fortran program, developed by Paul Fredrickson, determines the furthest range at which threshold signal strength for 90% probability of detection (POD) exist at the target elevation. This threshold is pre-determined and based on radar and target characteristics. The Advanced Refractive Prediction System (AREPS) was used to determine this

threshold value. Finally the field of ranges for each point is color contoured and a Portable Network Graphics (png) graphic is created as the final product similar to what is shown in Figure 13.

C. COMPARISON OF VALIANT SHIELD 2007, COAMPS[®] DATA AND BULK DATA FOR EVAPORATION DUCT

Continuous in-situ measurements were made throughout the VS07 exercise and were compared to the COAMPS[®] parameters. Figure 14 displays the time series for air temperature, sea temperature, wind direction and pressure. Figure 15 displays the EDH, ASTD, relative humidity and wind speed. The data presented in blue are the in-situ "truth" data and red are the 24-hour forecasts fields from COAMPS[®]. A preliminary comparison of both data sets show that the "truth" SST is slightly cooler on the average than the COAMPS[®] fields and "truth" air temperature warmer than the COAMPS[®] fields. All evaluations of VS07's METOC data will be examined and documented in future studies.

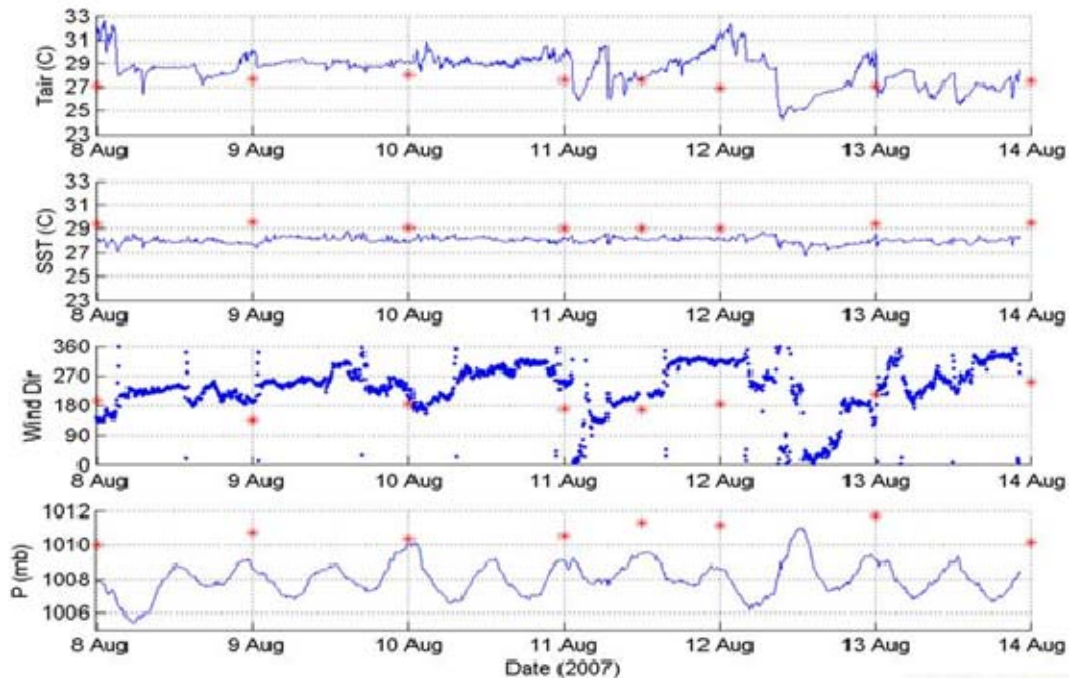


Figure 14. 8 August to 14 August 2007 RV Cory Chouest in-situ (blue) and COAMPS® time series (red dots) comparisons for air temperature (Tair), sea surface temperature (SST), wind direction (Wind Dir) and pressure (P).

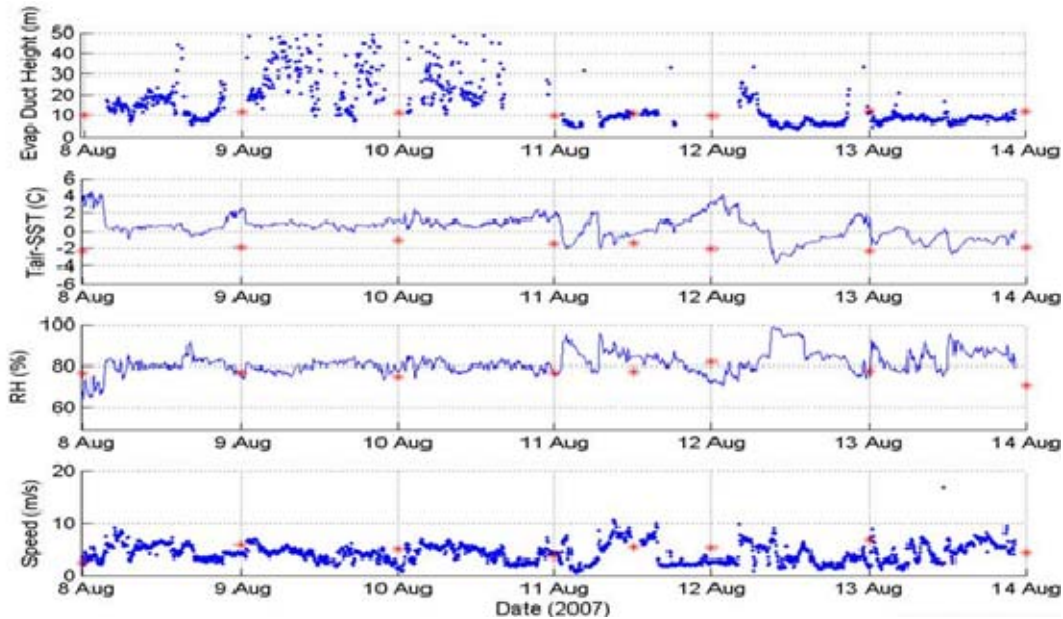


Figure 15. 8 August to 14 August 2007 RV Cory Chouest in-situ (blue) and COAMPS® (red) time series comparisons for evaporation duct height (EDH), ASTD (Tair-SST), relative humidity (RH) and wind speed (Speed).

THIS PAGE INTENTIONALLY LEFT BLANK

V. RESULTS FROM TRUTH VERSUS CLIMATOLOGY & COAMPS® COMPARISONS

A. COMPARISONS OF DATA SOURCES APPLIED TO NPS BULK MODEL

The time series of the Wallops Island 2000 and Valiant Shield 2007 data sets are used for direct comparison to model data. In this section, the time series of the Wallops Island 2000 and climatology data are presented for direct comparison. The figures display air temperature, SST, wind direction, wind speed, pressure, relative humidity, ASTD and EDH. The EDH was calculated using the NPS bulk method.

1. Comparison of Wallops Island NPS Buoy and Climatology Data

This study considers climatology as a possible resource in case preferred “truth” or model predicted data are limited or not available. Weather events, which do not exist within climatologies, can cause significant variations of temperatures of air and sea and relative humidity from climatology. It is expected that results of comparisons between “truth” and climatology would be much different at other less dynamic locations or times of year than the Wallops Island region in the spring, April.

Figure 16 displays “truth” and climatology time series for the Wallops Island period of 5 April until 13 May 2000 of air temperature, SST, wind direction and pressure. These data show that using climatology doesn’t capture significant weather events therefore the temperature of air, sea and relative humidity errors are large and are not accurately depicted.

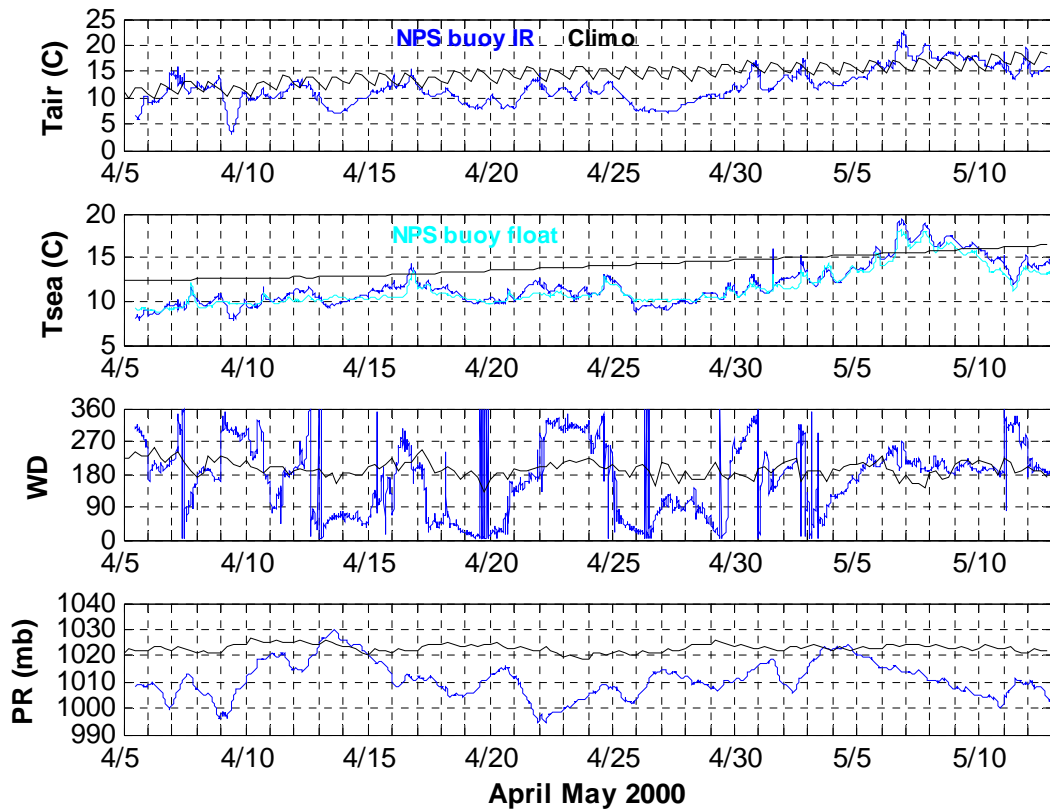


Figure 16. 5 April to 13 May 2000 NPS Buoy (blue) and Climatology (black) time series comparisons for air temperature (Tair), SST (Tsea), wind direction (WD) and pressure (PR).

Figure 17 displays “truth” and climatology time series for the same period shown in Figure 16 but for the calculated EDH and the parameters most closely associated with its value, RH of the air, wind speed, and air-surface temperature difference. The NPS bulk model was used to calculate the EDH.

“Truth” shows pronounced features of the EDH. These occur when calculated EDH values are large due to low RH values during times of low mixing, when Tair is greater than Tsea and the winds speeds are low. Another feature in the “truth”/buoy time series are times when EDH is zero (three-day period from 4/15-4/18), which is associated with sub-refractive conditions. This occurs when RH is equal or near to 100% and Tair is

greater than Tsea. The climatology time series does not show these occurrences, which is expected since its values represent average conditions.

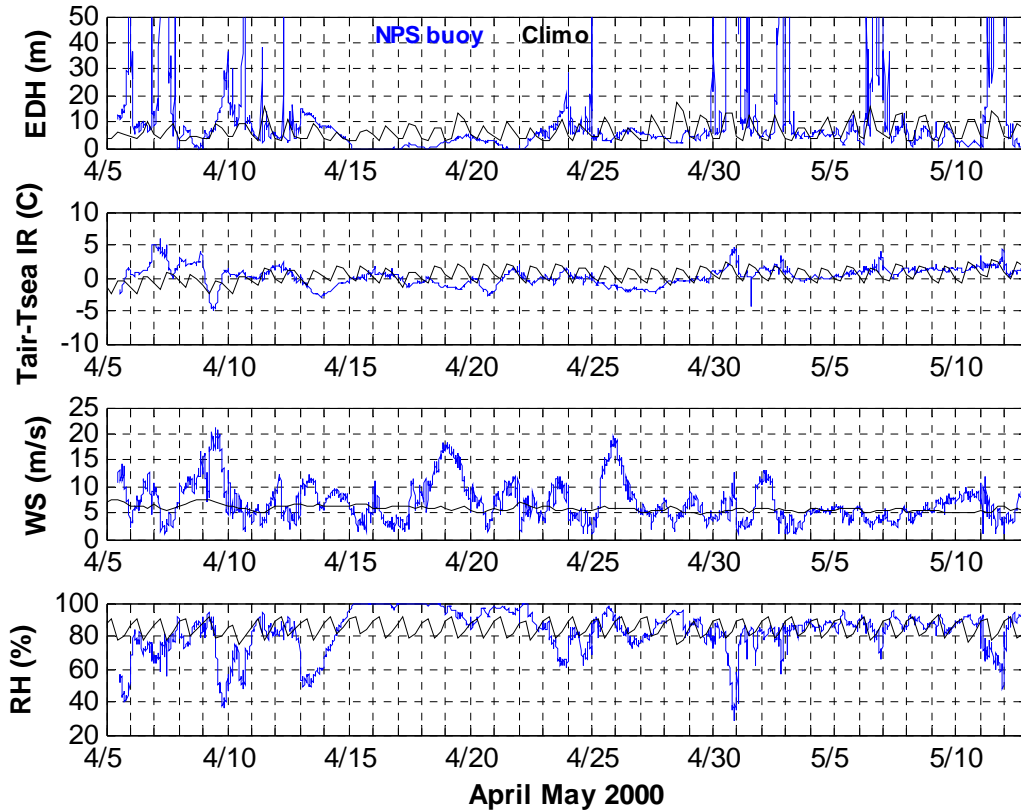


Figure 17. 5 April to 13 May 2000 NPS Buoy (blue) and Climatology (black) time series comparisons for evaporation duct height (EDH), ASTD (Tair-Tsea IR), Wind Speed (WS) and Relative Humidity (RH).

In order to compare METOC parameters of COAMPS[®] and climatology to “truth” data more closely, statistics generated from scatter plots give numerical values of correlated parameters. Figures 18-22 display the scatter plots for “truth”/buoy data and climatology.

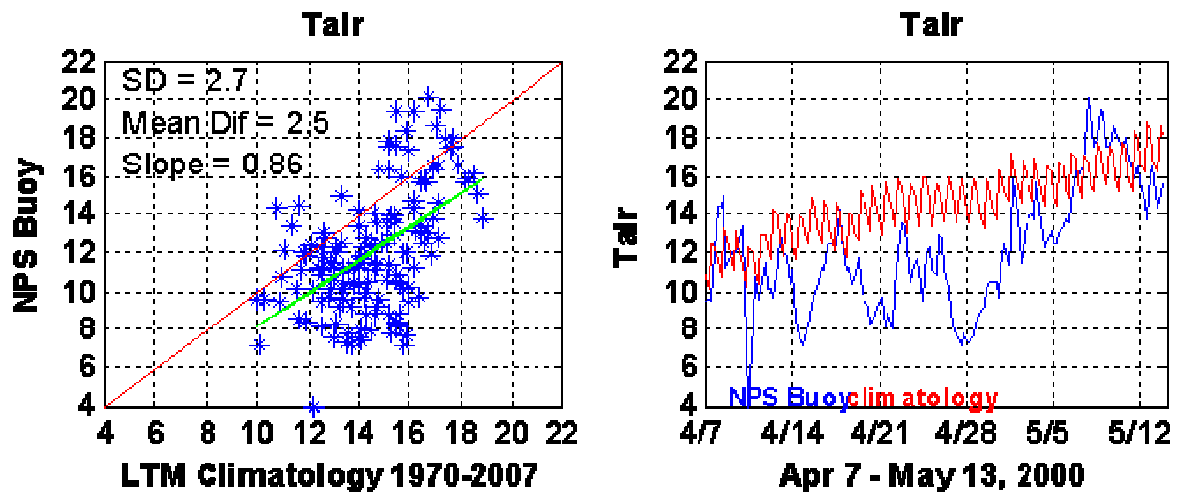


Figure 18. 5 April to 13 May 2000 NPS Buoy and climatology scatter plot and time series comparisons for air temperature (Tair).

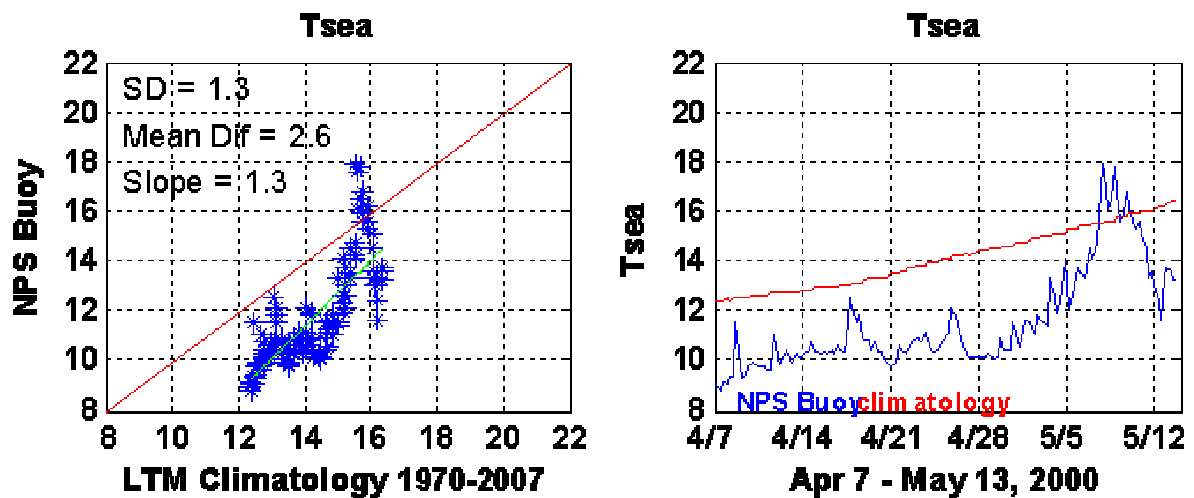


Figure 19. 5 April to 13 May 2000 NPS Buoy and climatology scatter plot and time series comparisons for SST (Tsea).

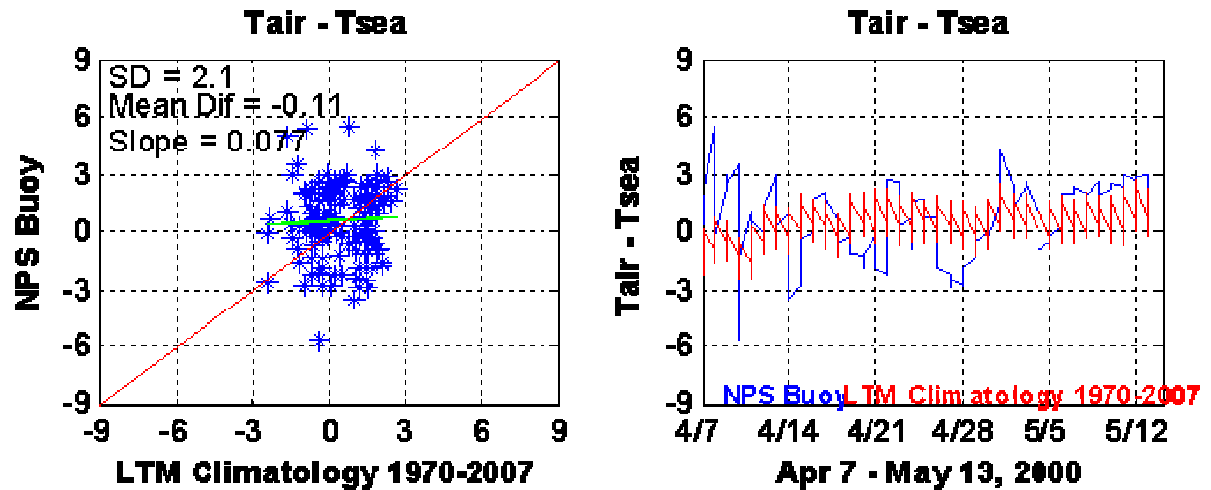


Figure 20. 5 April to 13 May 2000 NPS Buoy and climatology scatter plot and time series comparisons for air-sea temperature difference (Tsea).

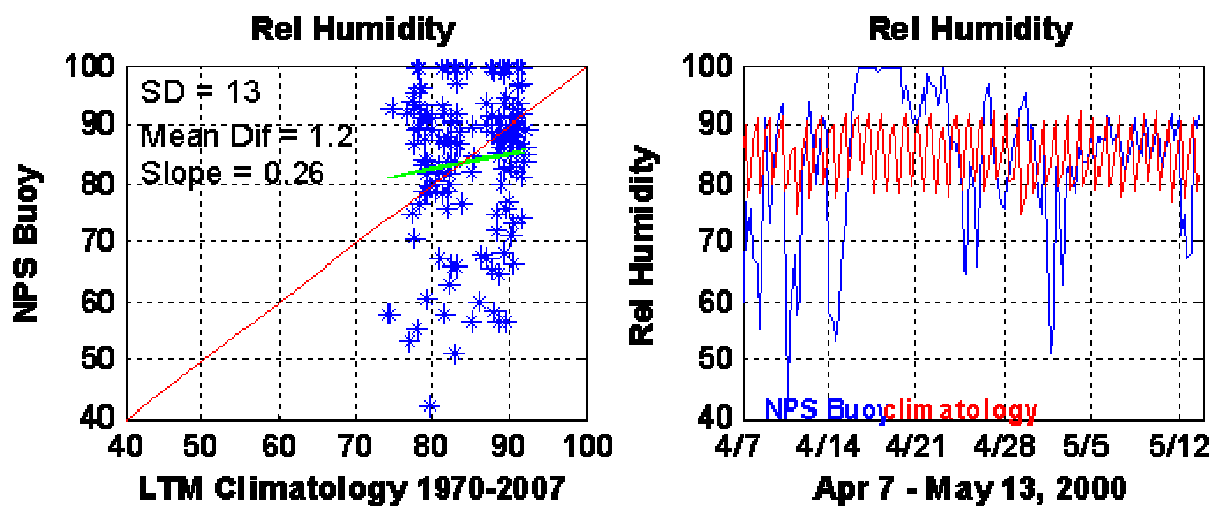


Figure 21. 5 April to 13 May 2000 NPS Buoy and climatology scatter plot and time series comparisons for relative humidity (Rel Humidity).

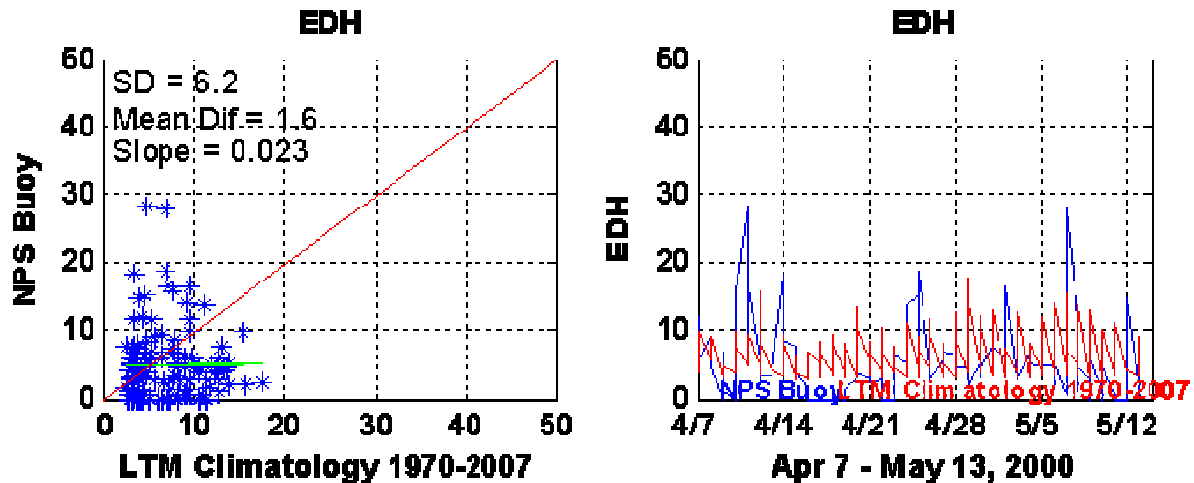


Figure 22. 5 April to 13 May 2000 NPS Buoy and climatology scatter plot and time series comparisons for evaporation duct height (EDH).

2. Comparison of Wallops Island NPS Buoy, COAMPS[®] Data and Evaporation Duct

Figure 23 displays “truth” and COAMPS[®] time series for the April and early May period, similar to the climatology time series. These comparisons indicate that COAMPS[®] predicts the forcing events adequately for operational uses on the basis of pressure, air temperature and wind direction, for the Wallops Island coastal regions and for a season that has mid-latitude system passages. The systematic variations were captured very well for these quantities. The pressure time series show COAMPS[®] and buoy data tracked each other fairly well as there is a 4 mb bias consistent throughout the time series. However, the COAMPS[®] SST time series shows, once initialized, it is held constant for 12 hours. This is different than the “truth” time series which has considerable variation. To evaluate the agreement closer, scatter plots of “truth” versus COAMPS[®] Tair, Tsea, Tair-Tsea, RH and EDU are shown in Figures 25-29. Scatter plot results indicate that COAMPS[®] Tair is within 1.5°C of “truth” and the RH is ~1 % off “truth,” on average. The scatter plot for Tsea shows higher values of COAMPS[®] when it is near 16°C.

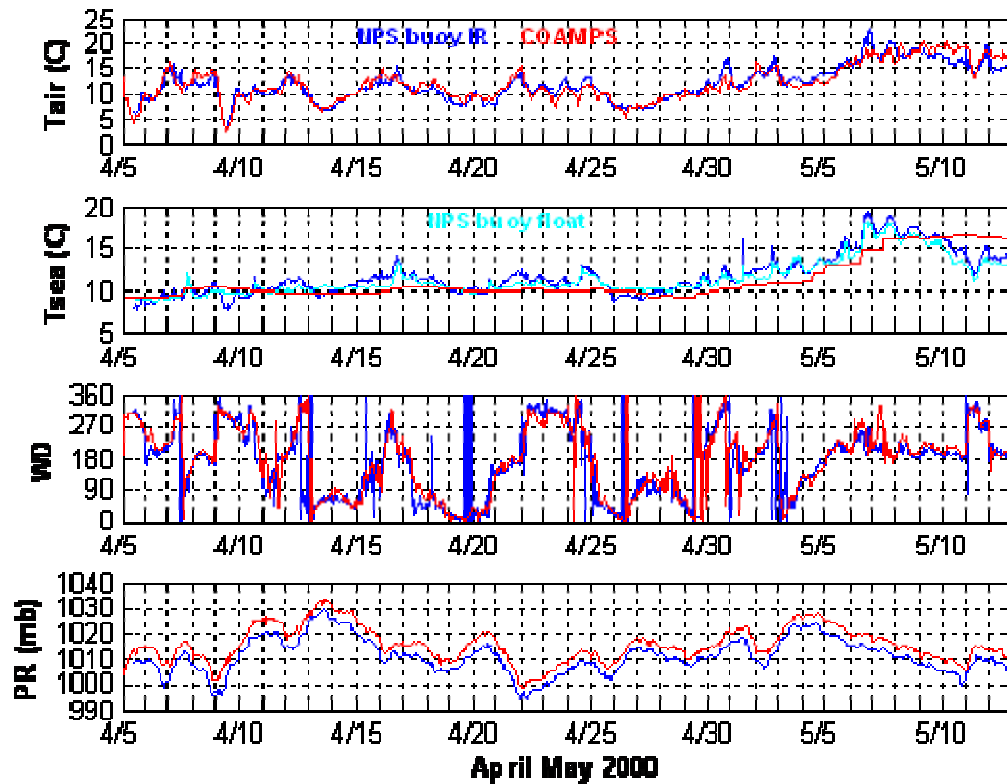


Figure 23. 5 April to 13 May 2000 NPS Buoy (blue) and COAMPS[®] (red) time series comparisons for air temperature (Tair), SST (Tsea), Wind Direction (WD) and Pressure (PR).

Figure 24 display "truth" /buoy and COAMPS[®] evaporation duct height (EDH) and the parameters most closely associated with its value, Tair-Tsea, RH, and wind speed. The latter two (RH and wind speed) show reasonable agreement over most of the time series. The ASTD of COAMPS[®] and buoy do not track well. This is primarily driven by differences in sea surface temperatures. The EDH differences are primary caused by the difference of air and sea temperatures.

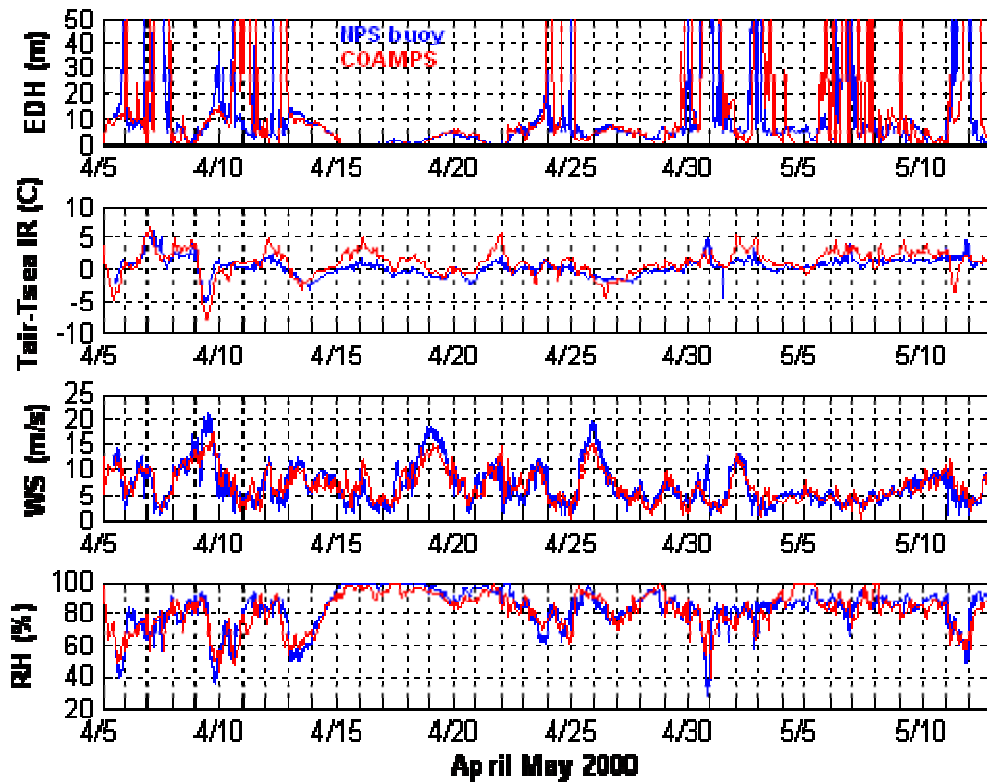


Figure 24. 5 April to 13 May 2000 NPS Buoy (blue) and COAMPS® (red) time series comparisons for evaporation duct height (EDH), ASTD ($T_{air}-T_{sea}$ IR), wind speed (WS) and relative humidity (RH).

Figure 25 displays a consistent correlated pattern of air temperature (T_{air}) for “truth” and COAMPS®. Statistics of air temperature show relatively good correlation throughout the entire period with a standard deviation (SD) of 1.3 and mean difference (Mean Dif) of 0.04.

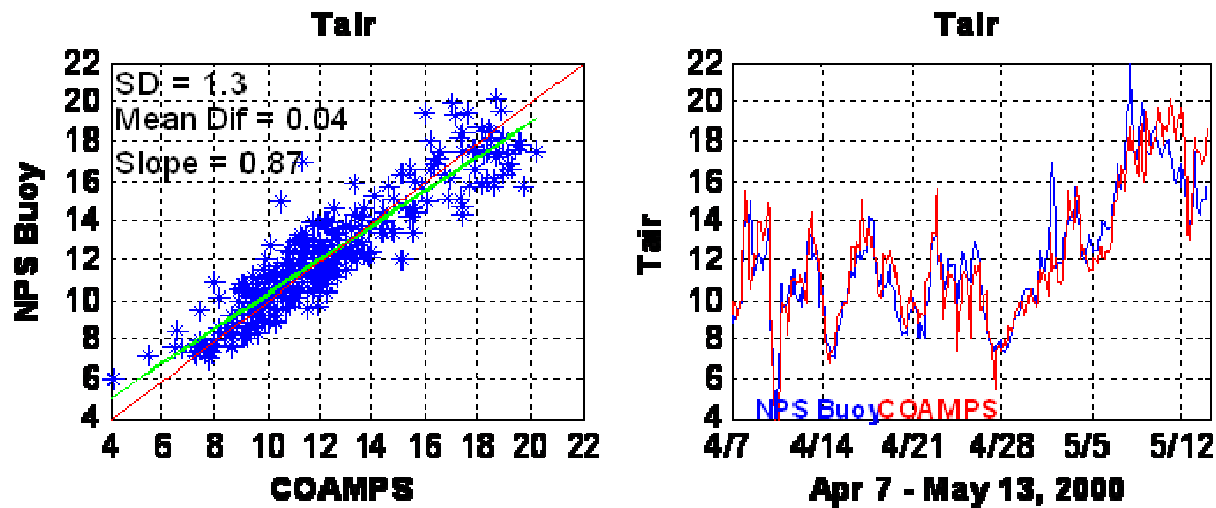


Figure 25. 5 April to 13 May 2000 NPS Buoy and COAMPS[®] scatter plot and time series comparisons for air temperature (Tair).

Figure 26 displays statistical correlation of sea temperature (Tsea) for “truth” and COAMPS[®]. COAMPS[®] makes greater errors in higher temperatures greater than 16°C. Statistics of air temperature shown throughout the entire period are standard deviation (SD) of 1.3 and mean difference (Mean Dif) of -0.34.

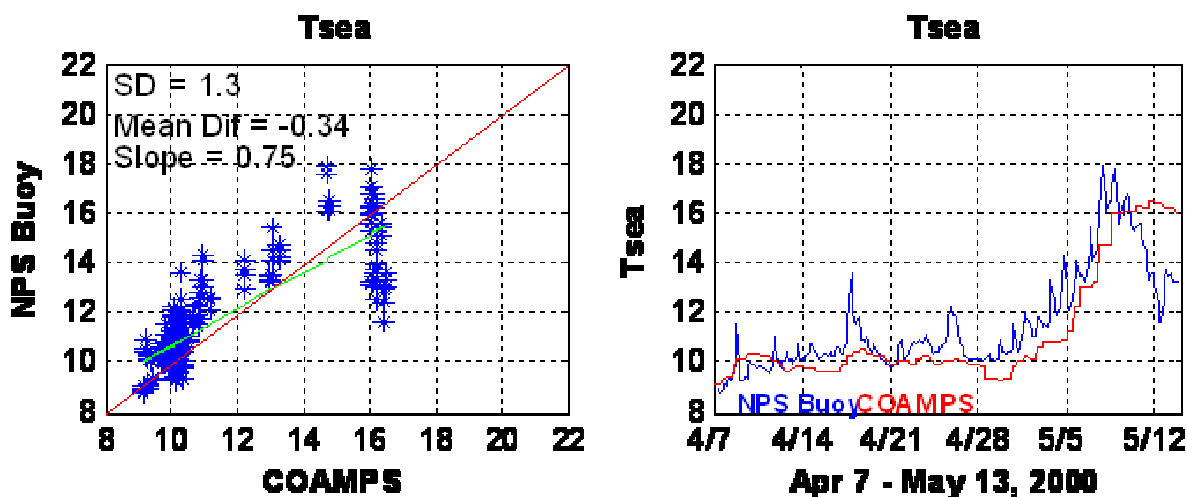


Figure 26. 5 April to 13 May 2000 NPS Buoy and COAMPS[®] scatter plot and time series comparisons for SST (Tsea).

Figure 27 displays consistent correlated pattern of relative humidity (Rel Humidity) for “truth” and COAMPS®. Statistics of relative humidity show good correlation with “truth” at higher humidity above 80% and less correlation below 80% in lower humidity.

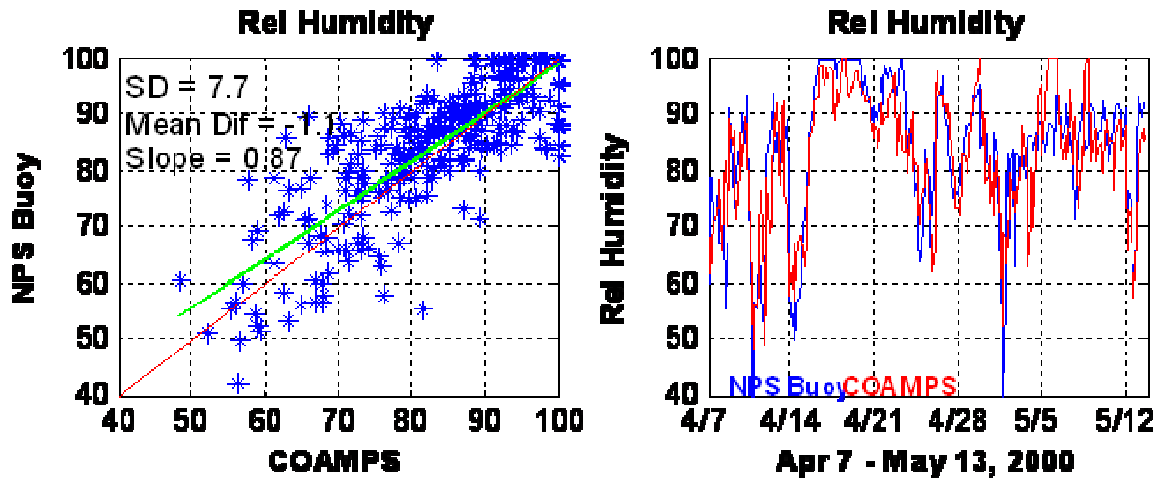


Figure 27. 5 April to 13 May 2000 NPS Buoy and COAMPS® scatter plot and time series comparisons for relative humidity (Rel Humidity).

Figure 28 displays statistical correlation of air-sea temperature difference (ASTD) for “truth” and COAMPS®. COAMPS® and buoy data are closely correlated when the ASTD is positive. At negative ASTD, COAMPS® seems to over estimate the swings in temperature.

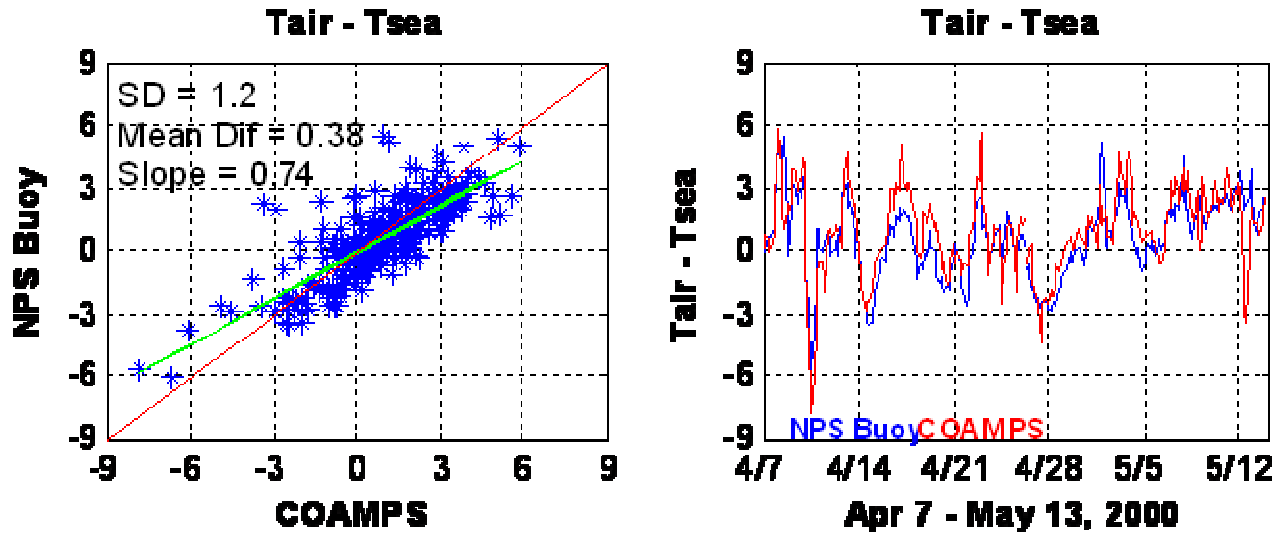


Figure 28. 5 April to 13 May 2000 NPS Buoy and COAMPS[®] scatter plot and time series comparisons for air-sea temperature difference.

Figure 29 displays a poor statistical correlation of EDH for “truth” and COAMPS[®]. This is due to sensitivities in the ASTD.

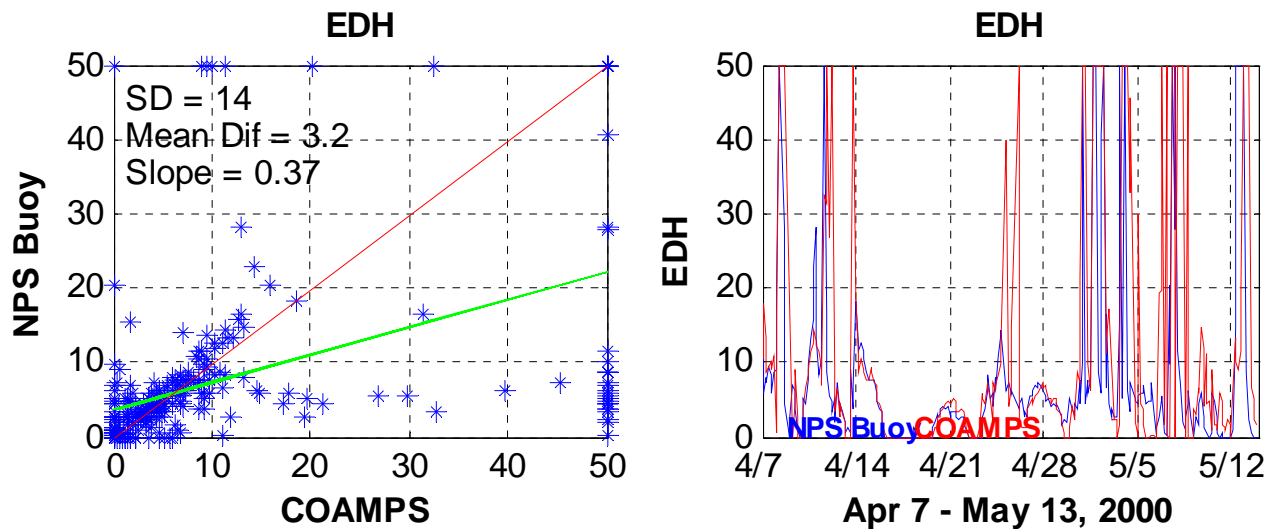


Figure 29. 5 April to 13 May 2000 NPS Buoy and COAMPS[®] scatter plot and time series comparisons for evaporation duct height (EDH).

Clearly there are varying atmospheric conditions throughout the full time series to cause EDH to fluctuate. EDH cannot be the deterministic or most absolute answer to

predicting ducting phenomena. The shape of the M profile with height up to and above that minimum value of M can be significant in explaining the strength of the duct.

The scatter plots produced compare climatology versus buoy (climatology minus buoy) and COAMPS[®] versus buoy (COAMPS[®] minus buoy). The standard deviation is equal to the square root of the mean of the squares of the deviations from the arithmetic mean. Table 3 summarizes the statistics drawn from the scatter plots comparisons.

METOC PARAMATER	STATISTIC	COAMPS [®]	CLIMATOLOGY
Tair (°C)	Mean Difference	0.04	2.5
	Standard Deviation	1.3	2.7
Tsea (°C)	Mean Difference	-0.34	2.6
	Standard Deviation	1.3	1.3
ASTD (°C)	Mean Difference	0.38	1.2
	Standard Deviation	1.2	13
RH (%)	Mean Difference	-1.1	1.2
	Standard Deviation	7.7	13
EDH (m)	Mean Difference	3.2	1.6
	Standard Deviation	14	6.2

Table 3. Statistic summary of METOC parameters with “truth” data.

B. METEOROLOGICAL SITUATION FOR MAY 11, 2000

As described, there were numerous days that had “truth” measurement and COAMPS[®] data extending from April 5 to May 13. 11 May 2000 was examined in detail due to the clear dissimilarities in air and sea temperatures between COAMPS[®] and “truth”.

On 11 May 2000, a mid-latitude cyclone moved through the mid eastern United States of Maryland, Pennsylvania and Virginia. A cold front associated with the cyclone appears in Figures 30 and 31 for 0015UTC and 0715UTC respectively, where at 0015UTC the front was west of Wallops Island and passage had occurred at 0715UTC. Applying the satellite cloud imagery to describe observed refractivity changing events is a way to show how satellites become part to the integrated approach/model shown in Figure2.

Wallops Island experienced warm moist air advection of prefrontal weather conditions at 0000UTC and cold dry air advection in postfrontal conditions at 0700UTC. The stability of the lower atmosphere is positive at 0700UTC as indicated by a +1.5 ASTD (Figure 33). Prefrontal relative higher humidity of 90 % is due to overrunning of warm moist air advected from synoptic southerly flow. Wallops Island experienced postfrontal weather conditions of relatively cold dryer air being brought into the area by a synoptic northwesterly flow. It will be seen that postfrontal lower relative humidity, below 70%, influences the Wallops Island at 0700UTC

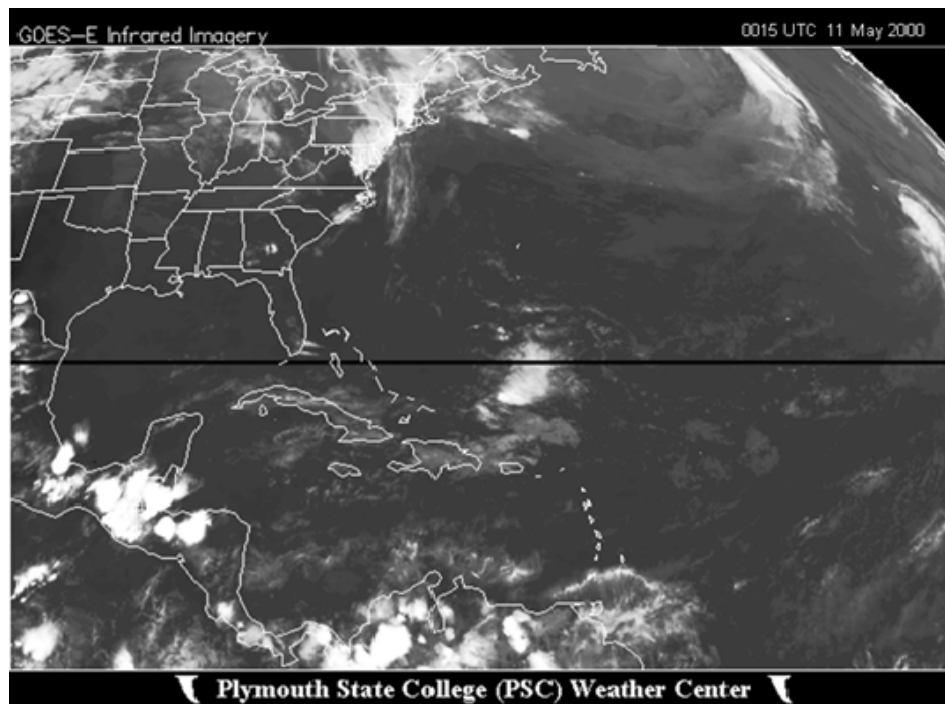


Figure 30. 0015UTC 11 May 2000 Infrared Imagery

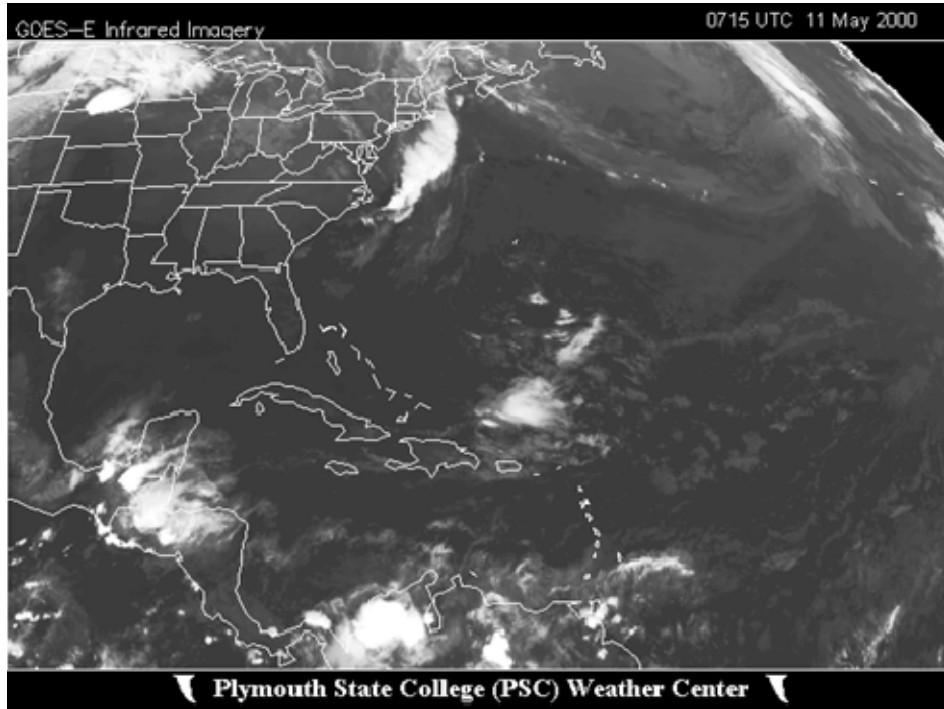


Figure 31. 0715UTC 11 May 2000 Infrared Imagery

Figure 27 displays “truth” and COAMPS[®] time series for the 11 May 11 2000 period of interest of air temperature, sea temperature, wind direction and pressure. At 0200UTC 11 May , the cold front moves through the Wallops Island area caused changes in wind direction, and in airflow and surface parameters, and hence, in near-surface refractivity conditions. The frontal passage caused air and sea temperatures and relative humidity to vary significantly between model data and “truth”.

In Figure 32, the period of cold frontal passage is circled and outlines the unchanging predicted COAMPS[®] sea temperature and the true cooling sea temperature captured by the flux buoy. The sequence of events was that warm moist air flows from the south over a colder underlying surface in the prefrontal air mass (0000UTC) on 11 May giving way to sub-refractive conditions. There is an apparent wind shift at 0200UTC where winds veer from southerly to northwesterly. The now offshore wind forcing off of Wallops Island causes colder ocean water to upwell and mix to the surface.

COAMPS[®] maintains its SST throughout the forecast period. “Truth”/buoy Tsea value decreased $\sim 3^{\circ}\text{C}$ with the frontal passage while the COAMPS[®] Tsea remained near-constant during it. The reason for the COAMPS[®] Tsea not decreasing is that it was not run as a coupled model and possibly have initialization issues as COAMPS[®] SST has no change through forecast.

As the postfrontal high pressure moves into area, the air temperature cools due to cold dry air advection from synoptic northwesterly flow. “Truth”/buoy Tair decreased $\sim 1^{\circ}\text{C}$ with the frontal passage event while COAMPS[®] Tair decreased $\sim 6^{\circ}\text{C}$. A primary outcome of the Tair-Tsea evolutions during the event was that the COAMPS[®] predicted Tair-Tsea became negative ($\sim -3^{\circ}\text{C}$), an unstable condition, while the “truth”/buoy Tair-Tsea remained positive ($\sim 2^{\circ}\text{C}$). The 0700UTC values correspond to the postfrontal air.

Both “truth”/buoy and COAMPS[®] relative humidity values in the prefrontal air mass (0000UTC) are 90% and drop to $\sim 70\%$ values in the postfrontal dry air mass. The COAMPS[®] airflow specific humidity, which is more directly responsible for the EDH than RH, would drop more since its Tair dropped.

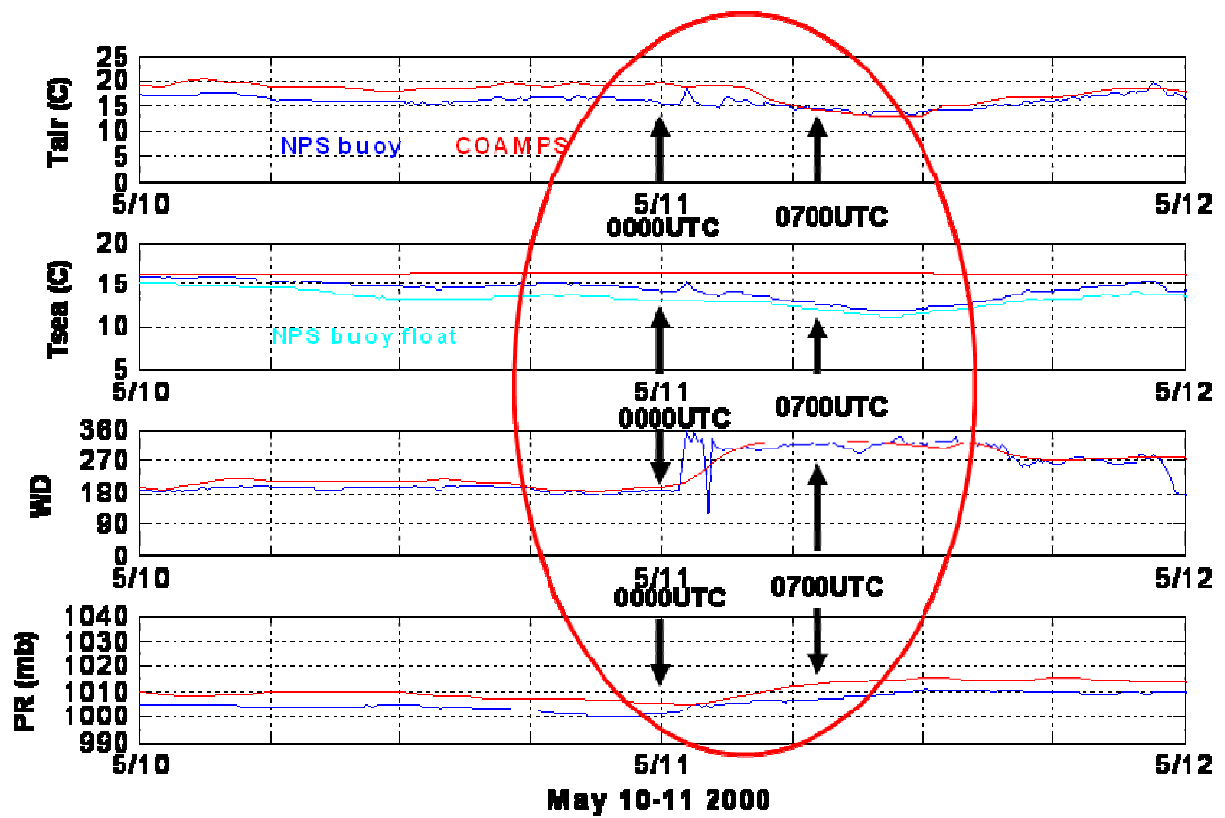


Figure 32. 10-11 May 2000 NPS Buoy (blue) and COAMPS® (red) time series comparisons for air temperature (Tair), SST (Tsea), wind direction (WD) and pressure (PR).

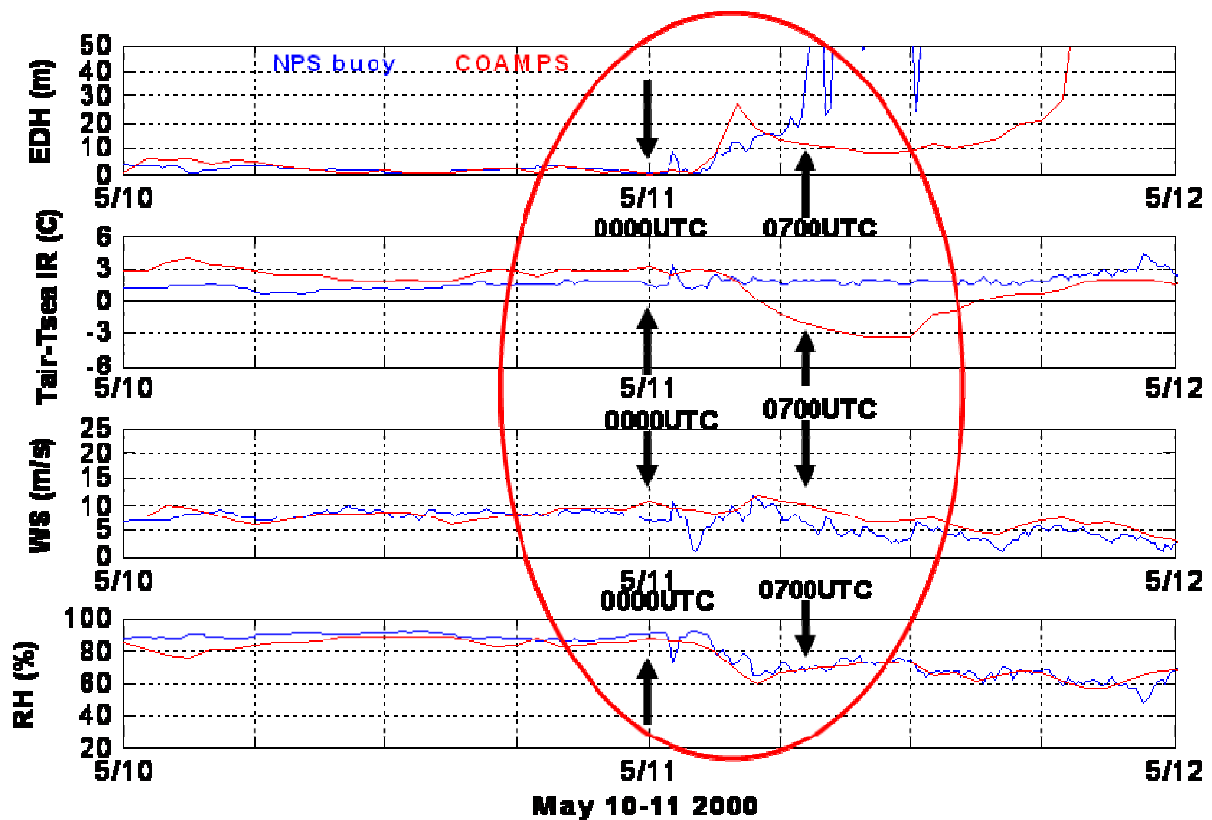


Figure 33. 10-11 May 2000 NPS Buoy (blue) and COAMPS[®] (red) time series comparisons for evaporation duct height (EDH), ASTD (Tair-Tsea IR), wind speed (WS) and relative humidity (RH).

Although the EDH is usually used to describe refractivity variations, as in the first row of Figure 33 it is useful to examine the refractivity profile, specifically the shape in gradient of M with height for ducting occurrences. Profiles were obtained from NPS bulk model calculations performed with “truth”/buoy and COAMPS[®] values as selected times on 11 May 2000. The wind speed, Tsea and EDH values differed significantly different between 0000UTC and 0700UTC. At 0000UTC, “truth”/buoy and COAMPS[®] looked similar with both having RH near 90% and positive Tair-Tsea value. However, the combined effects of the COAMPS[®] values, including airflow and Tsea lead to a sub-refractive layer, reported as EDH equal to 0 in Figure 34 and the “truth”/buoy having an

EDH near zero, but not sub-refractive (0000UTC). The profiles calculated by the NPS bulk model are shown in Figures 34 and 35 which displays the modified refractivity index, M, profile for 0000UTC and 0007UTC respectively. For 0700UTC, non-zero EDH's occurred for both the COAMPS® (~ 10m) and “truth”/buoy (~30m) data, which had much different Tsea values. This was due to the influence of extreme dryer cold air (RH ~69 %). The actual refraction conditions depend on the shape of the M profile rather than the EDH.

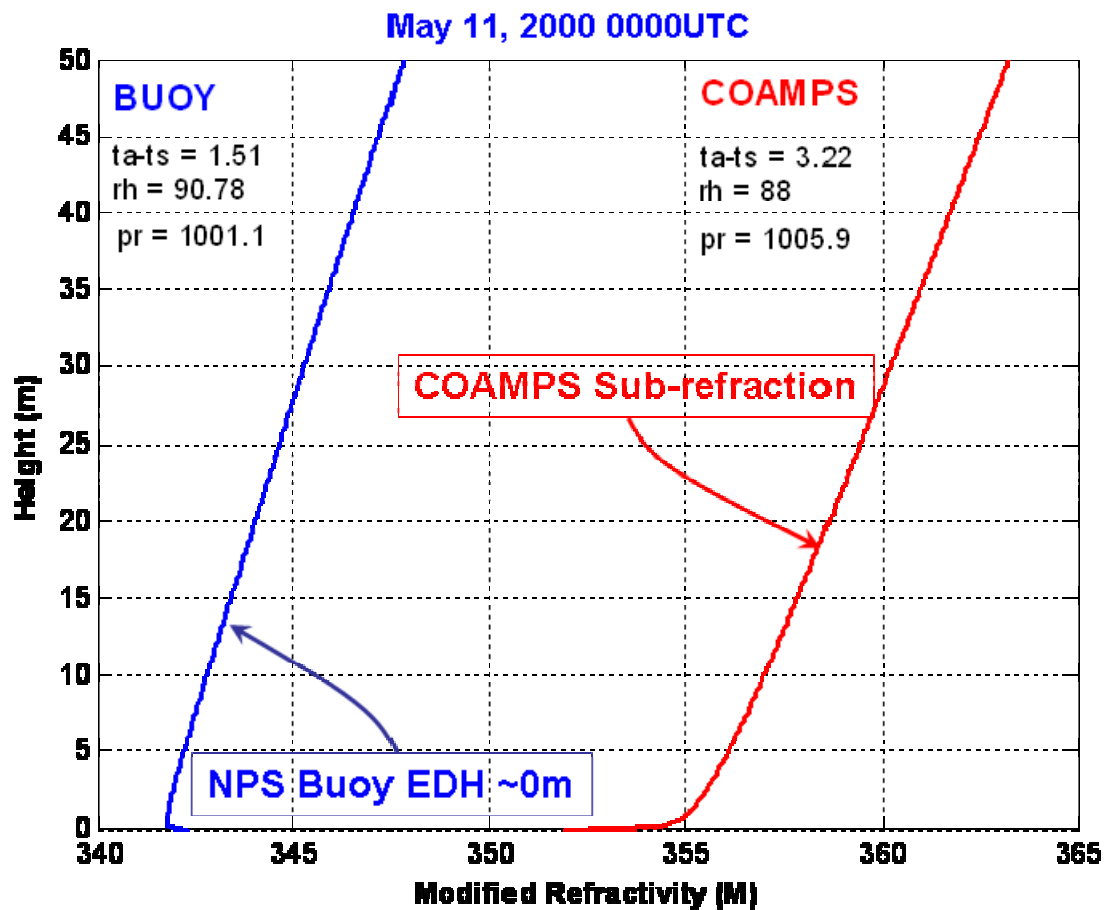


Figure 34. 0000UTC 11 May 2000 Modified Refractivity (M) with Height

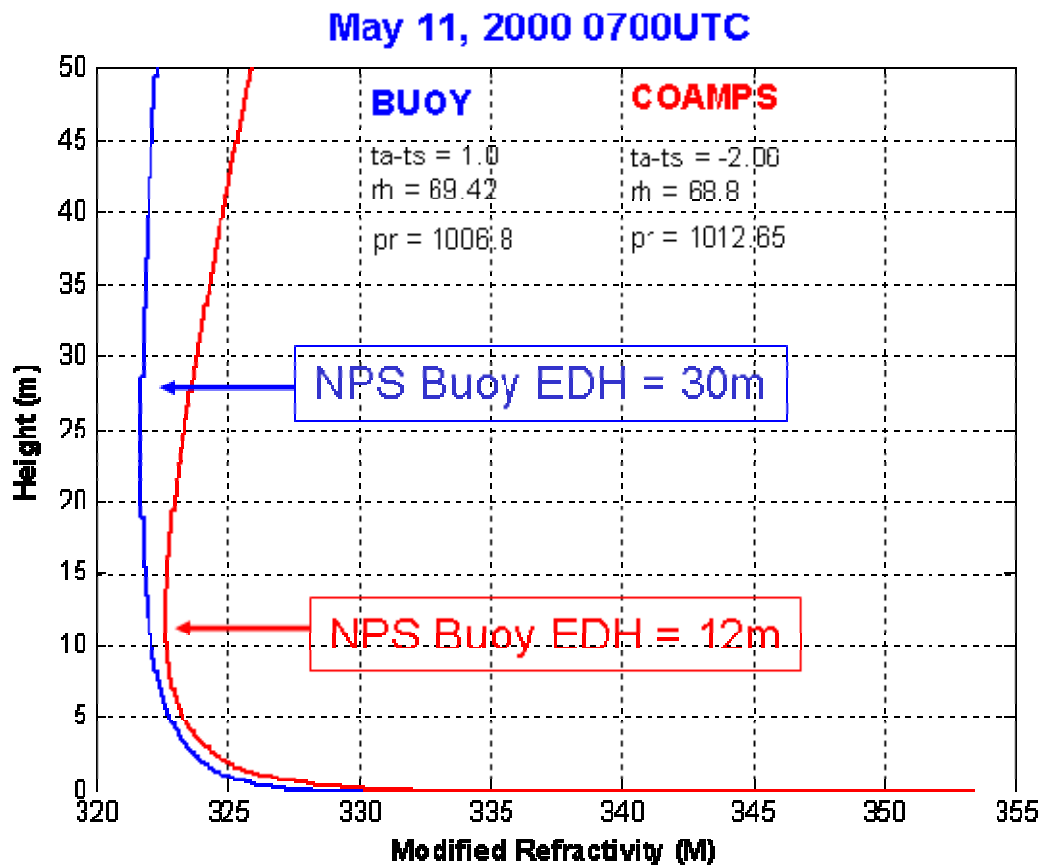


Figure 35. 0700UTC 11 May 2000 Modified Refractivity (M) with Height

C. PROPAGATION RESULTS

The gradient of M with height immediately above the surface influences the loss of radar detection capability of a low cross section target at the surface. The Advanced Propagation Model (APM) was used to calculate propagation loss (PL). All PL results shown in this section were for 10 GHz radar at 30 feet above ground level and a target at six feet above sea level (ASL) with a standard atmosphere range of 20 nm. The atmosphere was assumed to be homogeneous horizontally and APM was based on bulk values from “truth”/buoy and COAMPS® data, as well as a profile for the standard atmosphere.

Time series for PL at 20 nm for the entire period appear in the top panel of Figure 36 which is based on “truth”/buoy, and COAMPS[®] data derived profiles, and a standard atmosphere profile. The three time series, EDH, RH and Tair-Tsea, shown with PL shown to be the most influencing features. There is significant variation of PL associated with the changing influencing features. Compared to the standard atmosphere PL, The correlation between EDH and PL, with PL increasing as EDH decreasing, is apparent. For example, PL loss is more than 20 dB less than the standard atmosphere PL on 13 April and 80 dB greater than the standard atmosphere loss on 17 April. Hence, APM calculates that the influencing features caused a 100 dB change in the PL over four days. This time series comparisons suggests that the PL variation occurring over a few days is much larger than differences between PL’s calculated with “truth”/buoy, and COAMPS[®] data. However, closer examinations are useful. An examination of PL versus range (PL profiles) for same specifications as used for results in Figure 37 and 38 are made for the 0000UTC prefrontal conditions and for the 0700UTC conditions described above. The PL profiles for 11 May at 0000UTC and for 0700UTC appear in Figures 37 and 38, respectively.

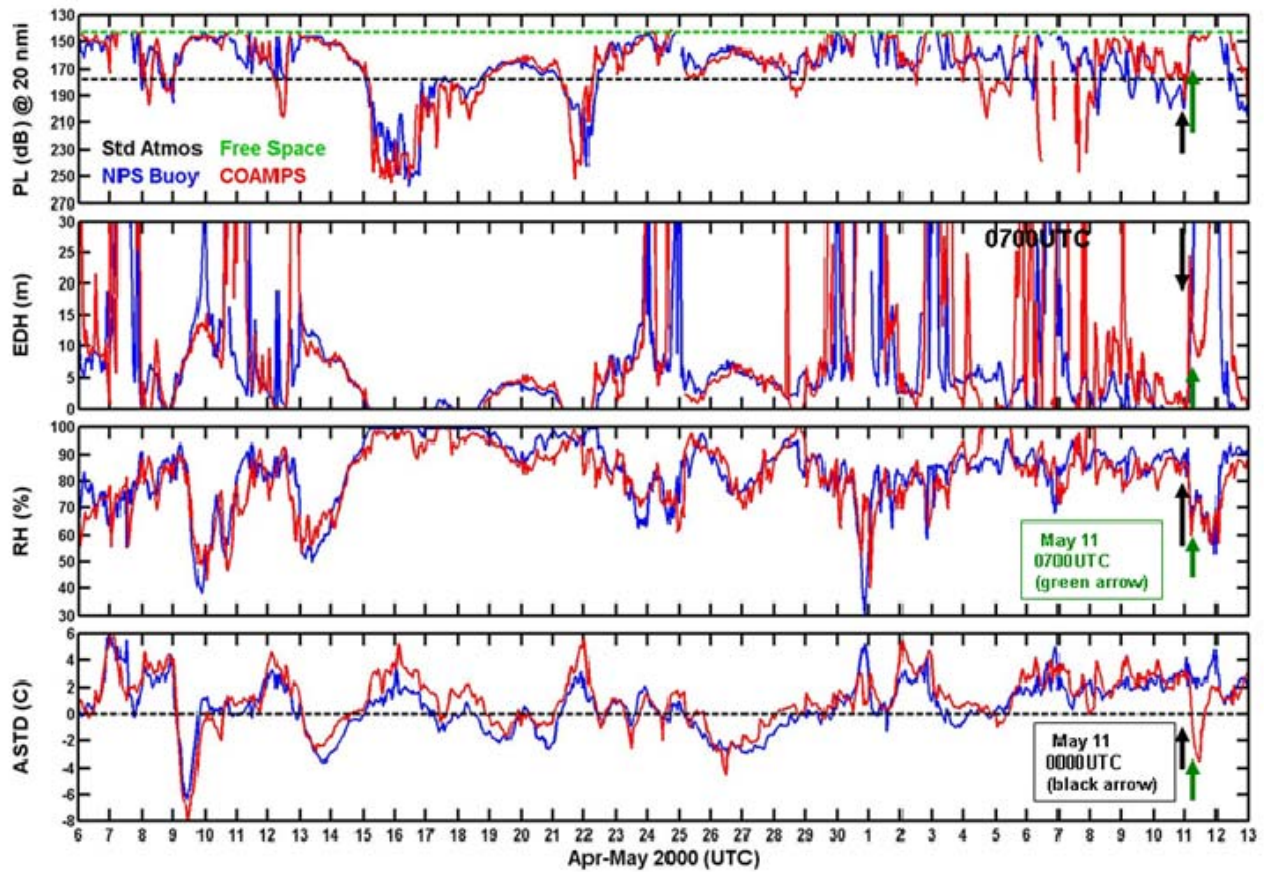


Figure 36. 6 April to 13 May 2000 NPS Buoy (blue) and COAMPS[®] (red) time series comparisons for propagation loss (PL), evaporative duct height (EDH), relative humidity (RH) and air-sea temperature difference (ASTD). Black arrows indicate 0000UTC and Green arrows indicate 0700UTC.

At 0000UTC, prefrontal conditions near sub-refractive EM propagation occurred where EDH is approximately zero. Figure 33 displays greater propagation losses for both “truth”/buoy and COAMPS[®] data, than for a standard atmosphere, with nearly 195 dB loss at 20 nm.

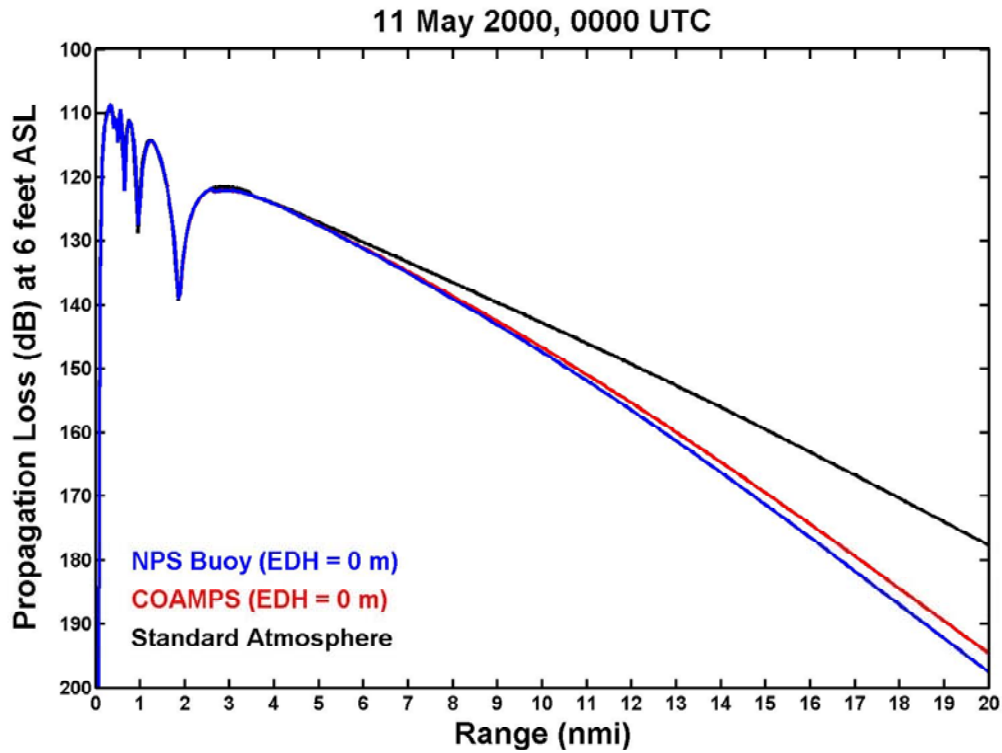


Figure 37. 0000UTC 11 May 2000 Propagation Loss Comparison, six feet above sea level (ASL), for NPS Buoy (blue), COAMPS[®] (red) and standard atmosphere (black).

At 0700UTC postfrontal weather conditions produced an evaporation duct giving extended EM propagation ranges. Figure 38 displays less propagation loss than that of a standard atmosphere with nearly 145 dB loss at 20 nm.

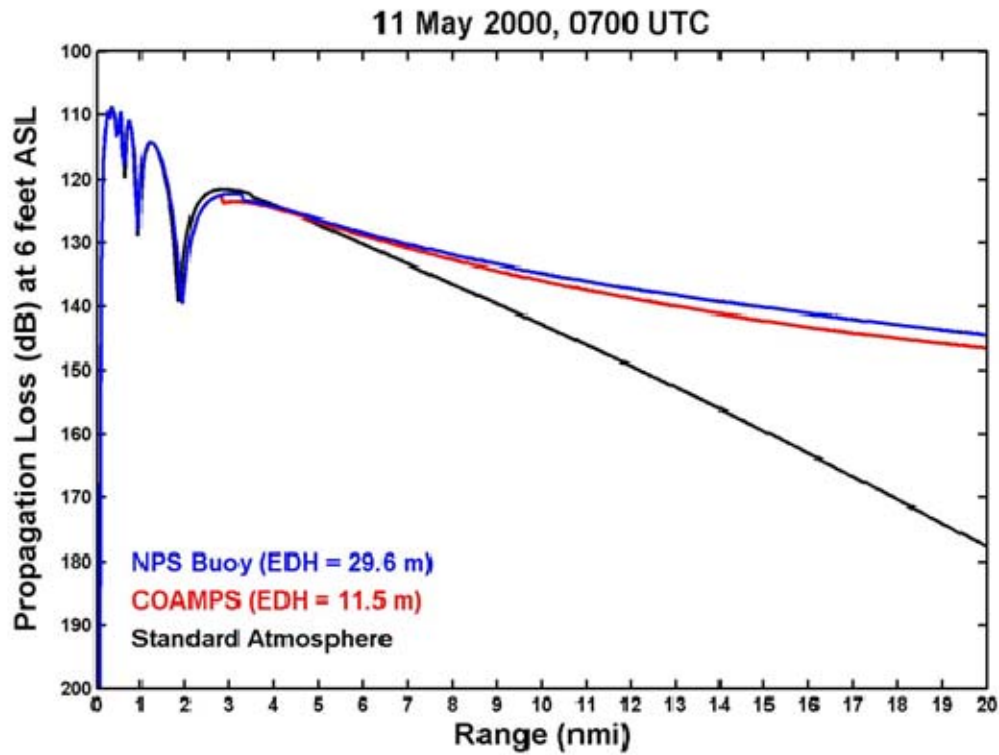


Figure 38. 0700UTC 11 May 2000 Propagation Loss Comparison, six feet above sea level (ASL), for NPS Buoy (blue), COAMPS[®] (red) and standard atmosphere (black).

The question often asked and an underlying aspect of all analyses/interpretations in this thesis is “how accurate do the near-surface measured and COAMPS[®] predicted parameters have to be, to be good enough?” One set of recommendations on accuracy and sensitivity for that question are presented in RHS of Table 4, (Davidson and Frederickson, 2006). The recommendation on sampling rate, accuracy and sensitivity have evolved from past and recent NPS surface-layer modeling, and atmosphere-based field tests carried out in conjunction with radar research and development and EO tests.

	Previous shipboard guidelines for Fluxes, EDH, and CNO 096 ORD			NPS guidelines for sub near-surface Accuracy & Sensitivity		
	Accuracy			Accuracy		Sensitivity
Parameter	SMOOS Blanc (1986) (Fluxes)	EDH-WS & Dockery (1995) (EDH)	CNO96 ORD Shipboard (1998) (MORIAH)	$\Delta T < 0$	$\Delta T > 0$	$\Delta T < 0$ & $\Delta T > 0$
Measurement Height	$\sim \pm 0.25$ m Analyses pertains to ~ 10 m			± 0.1 m Analyses pertain < 3 m		2 cm
Wind speed $\leq 20 \text{ ms}^{-1}$	± 0.5 m/s	10%	± 0.5 m/s	± 0.25 m/s	± 0.25 m/s	0.25 cm/s
Wind speed $> 20 \text{ ms}^{-1}$	± 1.0 m/s	10%	Not Considered	Not Considered	Not Considered	Not Considered
Air Temp	± 0.3 C	± 0.25 C	± 0.5 C	± 0.25 C	± 0.15 C	0.05 C
Wet Bulb temp	± 0.3 C	Not Considered	Not Considered	TBD	TBD	TBD
Relative Humidity	N/A	± 2 %	± 3 %	± 2 %	± 1 %	1%
SST	± 0.5 C	± 0.25 C	± 0.5 C	± 0.25 C	± 0.15 C	0.05 C
Pressure	Not considered	Not considered	± 1 hPa	± 1 hPa	± 1 hPa	0.5 hPa
Waves	Not Considered	Not Considered	Not Considered	TBD	TBD	TBD

Table 4. Comparison of accuracy values from different published guidelines appear in three separate columns on the LHS. Recommendations on accuracy and sensitivity for above listed data are provided in the RHS columns, from Davidson and Frederickson 2006.

This report is an initial step toward having an established metric for proper documentation of accuracies and sensitivities is imperative to gain confident answer the posed question. Future field test with an implemented metric will prove to be essential in knowing “*how good is good enough?*”

The sensitivities and accuracies of METOC parameters from model data does not meet guidelines outline in Table 4. However the above table has stringent sensitivity and accuracy requirements which in all likelihood could not be met in the near future by any numerical model. In fact COAMPS® performed well enough to be a valuable tool for predicting refractive conditions.

VI. SUMMARY AND CONCLUSION

A. SUMMARY

Statistics show, throughout the Wallops Island time series, COAMPS[®] predicted air and sea temperatures, relative humidity, pressure and winds showed considerable skill (Table 4). As seen on 11 May 2000, key differences between “truth” and COAMPS[®] data are in areas where transient mid-latitude frontal systems cause rapid changes in the air temperature, sea temperature and relative humidity. The greatest difference is in the SST field during this frontal passage. This is due to the lack of coupling in COAMPS[®] between the ocean and atmosphere and its subsequent consistent SST throughout the forecast. COAMPS[®] shows considerable skill in predicting propagation ranges before and after the frontal passage on 11 May 2000.

Although at different evaporation duct heights and different lower stability, COAMPS[®] and “truth” data both show ducting in postfrontal conditions (Figure 35). This was due to the presence of cold dry air (~69% RH) which was the principle reason for the ducting condition.

Fleet exercise Valiant Shield 2007 served as the “Proof of Concept” for the NPS’s Radar Performance Surface. The performance surface was developed, produced and distributed for operational use for the duration of the exercise. In situ measurements, on four different platforms in VS07, served to foster research and development in standardizing techniques to measure accurate air flow and sea skin temperature.

B. CONCLUSION

The development of the Radar Performance Surface was the driver for this research. The Radar Performance Surface was the “Proof of Concept” for fleet exercise Valiant Shield 2007. The end result of this development, the performance surface display, was presented to ASW operators during the exercise and was received well. The Radar Performance Surface successfully verified against positive contacts of submarine

periscopes in VS07. This leads to the conclusion that the impact of this concept to the warfighter proved to be a valuable tool. Further documentation and quantification of the impact will be necessary as the follow-on steps in the development occur. It is also concluded that incorporation of the Performance Surface requirements within FNMOC COAMPS production steps was successful. With regard to the next steps, the Wallops Island 2000 evaluation demonstrated that application of COAMPS, viewed as being critical as the input to the Performance Surface, was validated sufficiently to proceed with development along that line. Future collaboration among NPS, Navy Research Lab, Monterey and Fleet Numerical Meteorology and Oceanography Center is required and will merge and streamline current efforts to bring the Radar Performance Surface to the operational theater.

The sensitivities of the parameters that serve as the input to the performance surface were evaluated but not as substantial as necessary. Valiant Shield 2007 proved the SST is a difficult parameter to measure for shipboard operations. Infrared sensors represent a good promise for consistent method in measuring the SST (skin) temperature. A standard in capturing the skin's SST remains a challenge and will require further research and development.

LIST OF REFERENCES

- Anderson K., S. Doss-Hammel, C. Friehe, D. Hegg, T. Hristov, R. Janaswamy, H. Jonsson, and J. Reid, 2000: Mission Plan For The Rough Evaporation Duct (RED) Experiment, 27 pp.
- Babin, S. M., G. S. Young and J. A. Carton, 1997: A New Model Of The Oceanic Evaporation Duct. *J. Appl. Meteo.*, **36**, No. 3, 193-204.
- Baldauf, Brian K., 1996: Evaluation of Low Altitude Rocket Dropsondes for Shipboard Atmospheric Profiling and Electromagnetic Propagation Assessment, MS Thesis, Naval Postgraduate School, Monterey, CA, December 1996, 149 pp.
- Ballantine, S., 1928: The Lorentz reciprocity theorem for electric waves. *Proc. I.R.E.*, **16**, 513-518.
- Bean, B. R., and E. J. Dutton, 1968: *Radio Meteorology*. Dover Publications, New York, pp. 435.
- Call, D. B. 1994: LARDS A Low Altitude Rocket Dropsonde With PS Wind-Finding, Atmospheric Instrumentation Research Inc., Boulder, CO, 12 pp.
- Chief of Naval Operations, 2000: *Navy Strategic Planning Guidance With Long Range Planning Objectives*, 90 pp.
- Chief of Naval Operations (N096), 1999: *Navy Position on The Importance of Ocean Observations to Naval Operations*. [<http://oceanographer.navy.mil/Ocean-Obs-Statement.html>]. 05 April 2000.
- COAMPS[®] is a registered trademark of the Naval Research Laboratory Climate Diagnostics Center, Earth System Research Laboratory (ESRL), October 2005, [<http://www.cdc.noaa.gov/cdc/data.ncep.reanalysis2.gaussian.html>] September 2007.
- Climate Diagnostics Center Commander, Naval Meteorology and Oceanography Command, Strategic Plan, May 1997, [<http://www.cnmoc.navy.mil/pao.htm>]. 05 April 2000.
- Commander, Naval Meteorology and Oceanography Command, Battlespace On Demand Commander's Intent, May 2003, [<https://pao.cnmoc.navy.mil/pao/About%20Us/Battlespace.pdf>]. 18 November 2007.

- Davidson, K. L. and P. A. Frederickson, 2006: Environmental Data Collection for Estimating Atmospheric Impacts on Propagation from US Submarines, Report, prepared for CNMOC DOO ASW, 22 November 2006, 11 pp.
- Dockery, G. D., 1997: Meteorological Data Requirements For Assessment of Aegis Air Defense Capability. *Proceedings Electromagnetic/Electro-Optics Prediction Requirements & Products Symposium*, Naval Postgraduate School, Monterey, CA, 121-130.
- Derley, D. T., 2006: Remote Sensing of the Refractive Environment Above the Marine Stratocumulus-Topped Boundary Layer, M.S. Thesis, Naval Postgraduate School, Monterey, CA, 85 pp
- Fairall, C. W., E. F. Bradley, D. P. Rogers, J. B. Edson and G. S. Young, 1996: Bulk Parameterization Of Air-Sea Fluxes For Tropical Ocean-Global Atmosphere Coupled-Ocean Atmosphere Response Experiment. *J. Geophys. Res.*, **101**, 3747-3764.
- Frederickson, P., K. L. Davidson, F. K., 2006: Environmental Data Collection for Estimating Atmospheric Impacts on Propagation from US Submarines. Draft Memo, Naval Postgraduate School, Monterey, CA, 22 October 2006.
- Frederickson, P., K. L. Davidson, F. K. Jones, T. Neta, 2000a: Flux Buoy Data Report. Draft Memo, Naval Postgraduate School, Monterey, CA., 8 pp., 21 July 2000.
- Frederickson, P. A., K. L. Davidson, and A. K. Goroch, 2000b: Operational Bulk Evaporation Duct Model For MORIAH. Draft Memo, Naval Postgraduate School, Monterey, CA, 03 January 2000. 70 pp.
- Frieden, D. R., 1985: *Principles Of Naval Weapons Systems*, Naval Institute Press, Annapolis, MD, 27-88.
- Goldhirsh, J. and G. D. Dockery, 1997: Statistically Derived Propagation Factor Errors for the Mid-Atlantic Coast Region Due to Assumption of Lateral Homogeneity of Atmospheric Refractivity. *Proceedings Electromagnetic/Electro-Optics Prediction Requirements & Products Symposium*, Naval Postgraduate School, Monterey, CA, 121-130.
- Hitney, H. V., Refractive Effects from VHF to EFH, Part B: Propagation Models. Naval Command, Control and Ocean Surveillance Center Report, September 1994, 4B1-18.
- Hodur, R. M., 1996: The Naval Research Laboratory's Coupled Ocean/Atmosphere Mesoscale Prediction System (COAMPS®). *Monthly Weather Review*, **125**, 1414-1430.

- Lygre, A., and H. E. Krogstad, 1986: Maximum Entropy Estimation Of The Directional Distribution In Ocean Wave Spectra. *J. Phys. Oceanogr.*, **16**, 2052-2060.
- Derley, D. T, 2006: Remote Sensing of the Refractive Environment Above the Marine Stratocumulus-Topped Boundary Layer, M.S. Thesis, Naval Postgraduate School, Monterey, CA, 85 pp
- McBride, M. B., 2000: Estimation of Stratocumulus-topped boundary layer depth using sea surface and remotely sensed cloud-top temperatures. M.S. Thesis, Naval Postgraduate School, Monterey, CA, 101 pp.
- Murphy, Richard M. 2005 Analysis Of High-Resolution COAMPS® TM With Observed METOC Data To Demonstrate Atmospheric Impact On EM Propagation. Naval Postgraduate School, Monterey, CA, pp. 24-38.
- Nisley, W. H., 2000: Automated Meteorological And Oceanographic Data Collection And Distribution In Support Of C⁴I, Weapons, And Remote Sensing Systems, M.S. Thesis, Dept. of Meteorology, Naval Postgraduate School.
- Naval Surface Warfare Center, 2000: Site Test Plan And Procedures For The Microwave Propagation Measurement Experiment At The Surface Combat Systems Center (SCSC) Wallops Island Test Facility, Naval Surface Warfare Center (NSWC), Dahlgren, VA., 36 pp.
- Space and Naval Warfare Systems Command 2000: *User's Manual (UM) for Advanced Refractive Effects Prediction System Version 2.0*, Draft, Space and Naval Warfare Systems Command, METOC Systems Program Office (SPAWAR PMW-185), San Diego, CA.
- Wintronics, Inc, Selection Guide: Infrared Radiation Pyrometer KT15-IIP-Series 2004 [<http://www.wintron.com/Infrared/kt15iip/kt15iip.html>] May 2007.

THIS PAGE INTENTIONALLY LEFT BLANK

INITIAL DISTRIBUTION LIST

1. Defense Technical Information Center
Ft. Belvoir, Virginia
2. Dudley Knox Library
Naval Postgraduate School
Monterey, California
3. The Oceanographer of the Navy
United States Naval Observatory
Washington, DC
Attn: CAPT C. Gunderson
4. Kenneth L. Davidson
Meteorology Department, Code MR/DS
Naval Postgraduate School
Monterey, California
5. Peter Guest
Meteorology Department, Code MR/GS
Naval Postgraduate School
Monterey, California